FINAL REPORT

SOLID STATE MICROWAVE SOURCE DEVELOPMENT PROGRAM

Contract NAS8-25847

June 1971

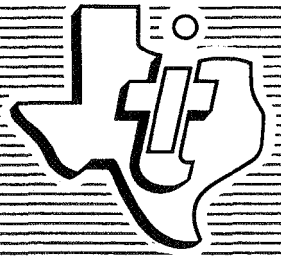

TEXAS INSTRUMENTS
INCORPORATED

FINAL REPORT

SOLID STATE MICROWAVE SOURCE DEVELOPMENT PROGRAM

Contract NAS8-25847

June 1971

Prepared for

NATIONAL AERONAUTICS AND SPACE ADMINISTRATION

Marshall Space Flight Center

Huntsville, Alabama

by

W. R. Wisseman
H. Q. Tserng
D. W. Shaw
T. E. Hasty

Texas Instruments Incorporated

TEXAS INSTRUMENTS
INCORPORATED

CORPORATE
RESEARCH &
ENGINEERING

13500 NORTH CENTRAL EXPRESSWAY P. O. BOX 5936 DALLAS, TEXAS 75222

FOREWORD

This report was prepared by Texas Instruments Incorporated, 13500 North Central Expressway, Dallas, Texas 75222 under Contract No. NAS8-25847, DCN 1-0-40-93877. It summarizes work performed from 31 May 1970 to 31 May 1971. Dr. D. O. Lowrey of the Astrionics Branch, NASA Marshall Space Flight Center, was project manager.

At Texas Instruments the program was carried out in the Microwave Physics branch of the Physics Research Laboratory, part of TI's Central Research Laboratories. Dr. T. E. Hasty was program manager, and Drs. W. R. Wisseman, H. Q. Tserng, and D. W. Shaw were major contributors to the work reported here.

Texas Instruments report number is 08-71-38.

TABLE OF CONTENTS

LIST OF TABLES

TABLE OF CONTENTS

(continued)

LIST OF ILLUSTRATIONS

SECTION I

INTRODUCTION

This report summarizes work performed during the past 12 months at Texas Instruments under Contract No. NAS 8-25847 to develop a solid state microwave source which satisfies the transmitter requirements for a satellite communication system. The general capabilites desired are:

Frequency	C- to X-band
Power	1 watt cw
dc to rf efficiency	40% to 50%

We proposed to develop a microstrip oscillator with an ultimate goal of satisfying all of these transmitter requirements; however, during the time frame of this contract we expected to deliver a microstrip oscillator which satisfied the frequency and power requirements, but operated at a lower efficiency level. We also hoped to lay the groundwork necessary to achieve the very high efficiency ultimately required. To meet these goals we chose to develop a GaAs avalanche diode which could be operated in microstrip. We planned first to operate the diode in the IMPATT mode, where efficiencies of 10 to 15% are possible. We next planned to operate the diode in the TRAPATT mode, where it is expected that efficiencies of 40 to 60% could be achieved.

At the beginning of the program, it was our opinion that only avalanche diodes operating in the TRAPATT mode could satisfy all the contract requirements. On the basis of the extensive work done at Texas Instruments on microwave transistors, Gunn and LSA diodes, and silicon avalanche diodes, we concluded that only silicon or GaAs avalanche diodes could achieve the required high efficiencies in the desired frequency range. GaAs avalanche diodes were selected because they operate at nearly twice the efficiency of silicon diodes in the classic IMPATT mode. Although TRAPATT operation has not yet been demonstrated for GaAs diodes, there appears to be no fundamental limitation which would prevent their operation in this mode.

The results of our efforts to meet the contract goals are summarized below.

(1) Developed required materials and fabrication technology.
(2) Achieved IMPATT operation in waveguide: 1.0 W at 9.0 GHz and 14.0% efficiency, 1.2 W at 9.0 GHz and 12.2% efficiency.
(3) Achieved IMPATT operation in microstrip: 0.81 W at 10.1 GHz and 11.0% efficiency (to be delivered).
(4) Completed preliminary design of TRAPATT circuitry.

The first part of this report presents a description of the device development phase of the program, including a brief discussion of the basic device structure, materials development, device fabrication, and evaluation. This is followed by a discussion of our circuit development work, which required an extensive device characterization effort prior to the design and testing of a microstrip oscillator. Finally, we summarize our results and suggest future directions for research. The appendix contains a description of how the GaAs Schottky barrier diodes developed for this program have been used to support Texas Instruments K_u-band Gunn local oscillator work for the government.

SECTION II

DEVICE DEVELOPMENT

A. Basic Device Structure and Operating Modes

The properties of avalanche diodes operating in both the IMPATT and the TRAPATT modes are well documented in the literature.[1,2] No attempt will be made here to give detailed descriptions of these modes, but some comments are necessary to point out basic differences is the structures and circuits required for optimum operation.

An avalanche diode is a junction device which is biased into reverse breakdown. Under certain conditions, it is possible at particular frequencies to get a phase shift between an rf voltage and its associated current which is greater than 90°. When this occurs, the device has a negative resistance at these frequencies, and it can be made to oscillate if presented with the proper circuit impedance. The reverse I-V characteristic and operating point for an avalanche diode are indicated in Figure 1(a).

The basic structure of an avalanche diode is illustrated schematically in Figure 1(b). We have shown a Schottky barrier diode rather than a p-n junction device because most of our work has been with the Schottky structure. The active n-layer is grown epitaxially on a heavily doped n^+ substrate which has an ohmic contact on the other side. The metal contact to the n-layer forms a rectifying Schottky barrier. The potential barrier at this contact arises from stable space charges in the semiconductor. When the device is reverse-biased, the width of the space charge region is increased as a result of electron depletion. This increase in depletion depth continues until the point at which thermally generated electrons in this depleted region acquire enough energy from the electric field to cause avalanche breakdown. The depletion depth at reverse breakdown, W_D, is indicated in the figure.

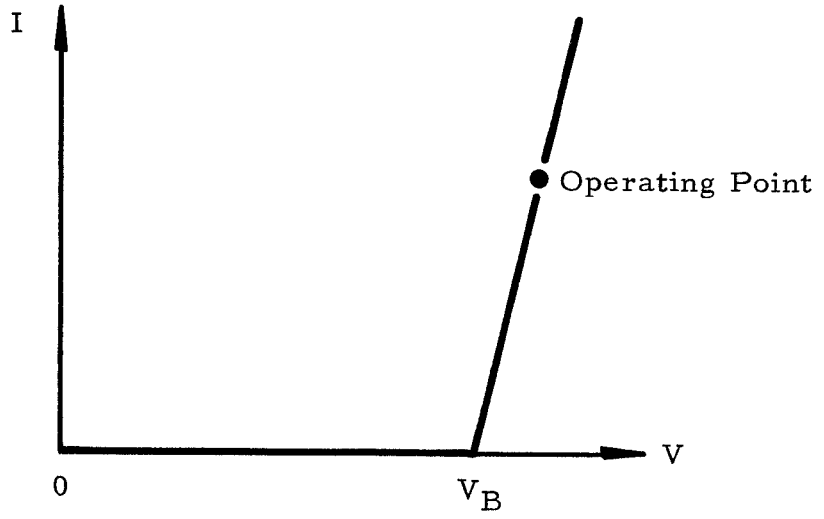

(a)

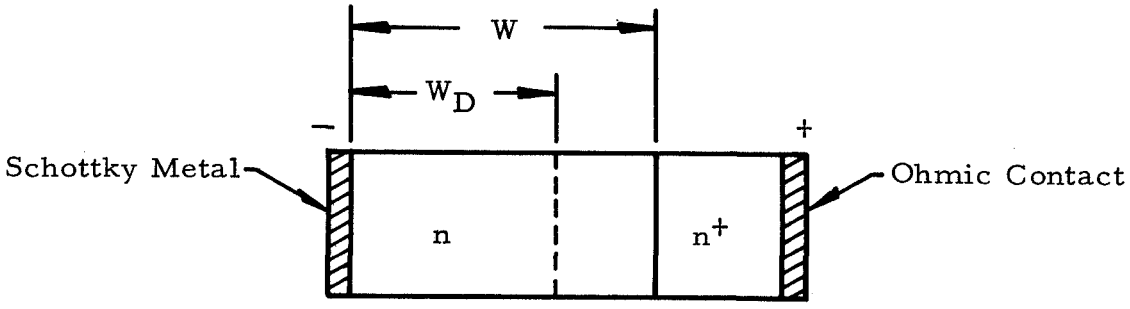

(b)

6915-18

Figure 1(a) Avalanche Diode Reverse I-V Characteristic
(b) Basic Avalanche Diode Structure

The IMPATT mode is a relatively stable mode of oscillation, and small and large signal theories have been developed.[1] The phase shift between rf voltage and current arises from both transit time effects and the basic avalanche mechanism. Most IMPATT diodes are designed so that $W_D \leq W$ because this reduces the chance of a tuning induced failure by introducing the series resistance of the undepleted region of length $W - W_D$. This series resistance also has the effect of decreasing the dc to rf conversion efficiency so that generally W_D is only slightly less than W. For optimum performance in the IMPATT mode, the diode must operate into a matched load. Since the device impedance is generally quite low, compared with a 50 Ω microstrip line, it is necessary to provide for an impedance transformation. Details of how this has been done are given in Section III of this report.

The TRAPATT mode is a high efficiency mode which can be treated only by large signal theories.[2] One requirement for TRAPATT operation which comes from large signal theory is that the n-layer must be fully depleted ($W_D = W$, "punch-through") because oscillation would be inhibited by the series resistance of an undepleted region. The frequency of TRAPATT oscillation is subharmonically related to the IMPATT frequency for the diode. The circuit requirements are more complicated than those for the IMPATT mode. Not only must the circuit be designed to match properly at the TRAPATT frequency, but it must also include provision for trapping harmonics of the TRAPATT frequency (including the IMPATT frequency) so that the proper waveform for high efficiency operation is impressed across the diode. There is a minimum threshold current density for the onset of this mode; consequently, devices are more susceptible to tuning failure, since they are already operating at a high power level when the TRAPATT threshold is reached.

B. Materials Preparation

Epitaxial GaAs layers used in this program were grown from the vapor using a $Ga/AsCl_3/H_2$ system similar to that developed at Texas Instruments for fabrication of Gunn effect diodes. Figure 2 is a diagram of the apparatus. It is constructed of fused silicon and surrounded by a two-zone furnace. The

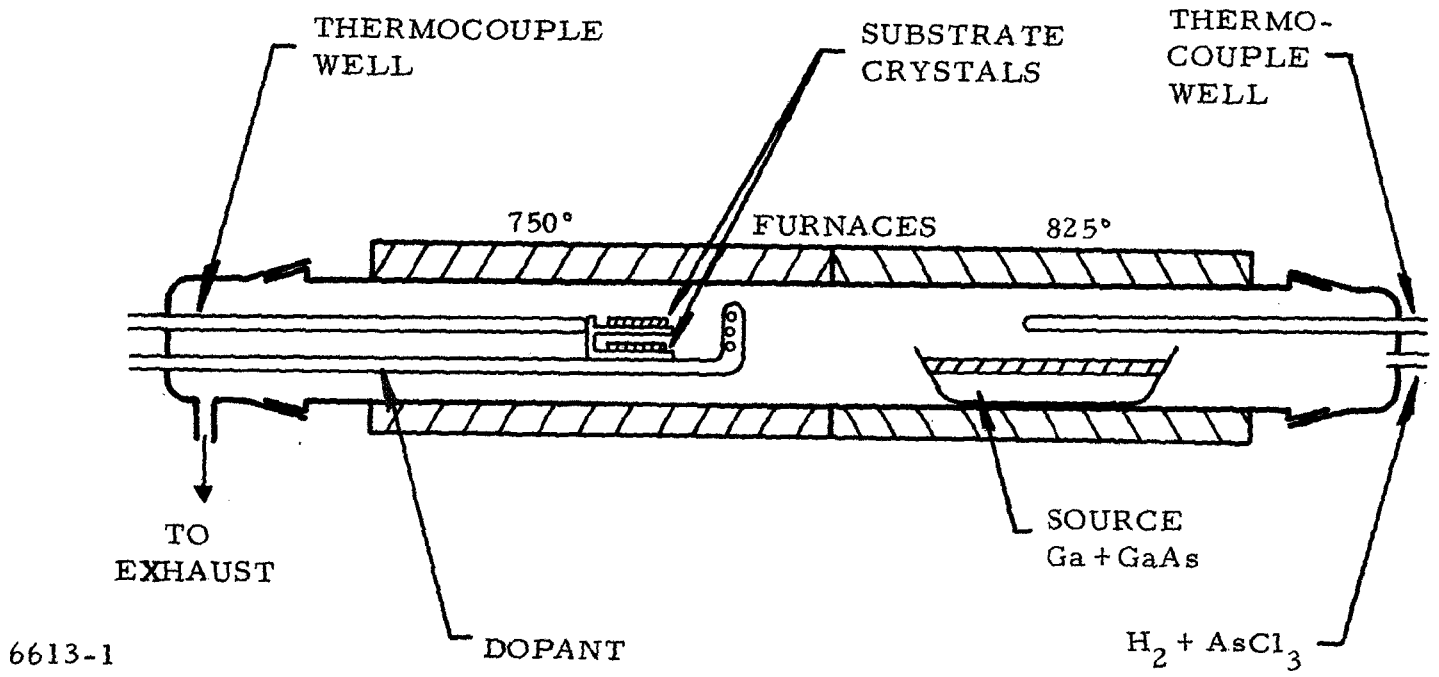

Figure 2 Epitaxial Growth Apparatus

source boat containing 99.9999% elemental gallium is situated in the higher temperature region. High purity (99.999%) $AsCl_3$ is passed over this source with Pd-diffused hydrogen as a carrier gas. Before epitaxial growth can occur, the gallium source must be saturated with arsenic until a thin crust of solid gallium arsenide forms on the surface. Recent studies[3] of source saturation and transport have revealed that attempts to grow epitaxial layers with an incompletely saturated source can result in large changes in gas phase composition. Since this phenomenon can lead to formation of high resistivity regions in GaAs, every effort was made to ensure complete source saturation. After the flowing gas stream passes over the source and becomes charged with reactants, it enters a lower temperature deposition region in which the substrate crystals are located. These substrates were cut from Te-doped GaAs ingots grown by the Czochralski technique. They were oriented 2° from the {001}. Provisions are made to dope the deposits by introducing a donor impurity just upstream from the growing crystals. The dopant is introduced at this point to prevent contamination of the source. This is particularly important when multiple layers are grown simultaneously, since relatively abrupt "junctions" are desired. The conditions were adjusted so that growth always occurred only on the substrate crystal and not on the substrate holder or surrounding parts. Extraneous deposits on the tube walls or substrate holder compete with the growing layers for reactants and lead to thickness and doping gradients over a slice.

Although the desired doping level for GaAs IMPATT devices is around 1×10^{16} cm^{-3}, every effort was made to first produce undoped epitaxial layers with concentrations below 10^{15} cm^{-3}. With this doping level, it is possible to intentionally dope the layers up to the desired value and consistently produce uniform deposits doped with a known impurity. All epitaxial layers used for IMPATT diode fabrication during this program were sulfur doped. Due to the nature of the device fabrication technique, it was also necessary to produce layers whose surfaces were very smooth and free from defects. With suitable control over deposition parameters this is rather easily achieved with the $Ga/AsCl_3/H_2$ system. In fact, surface quality and ease of doping are two important advantages of vapor phase epitaxy in comparison with solution or liquid phase epitaxy.

Initially, the layers were grown 3 μm thick. An example of a cleaved {110} cross section through a typical slice is shown in Figure 3. This cross section has been etched in a chromic oxide etchant[4] which reveals crystal defects. The difference in crystal quality between the epitaxial layer and the substrate is striking. No defects are apparent in the epitaxial layer, while a number of various types of imperfections are evident in the substrate. It is amazing that these substrate defects do not propagate into the epitaxial layer. Nevertheless, the epitaxial region immediately adjacent to the substrate must be strained. Poor device performance was often observed with thin layers such as these when the depletion region extended nearly to the substrate. It is possible to reduce this problem by growing thicker epitaxial layers ($\sim$ 10 μm). However, the excess epitaxial thickness also results in a high series resistance which is detrimental to device performance.

The substrate problem was essentially eliminated by growing two-layer structures such as those illustrated by the {110} cross section in Figure 4. In this case, the first epitaxial layer is relatively heavily doped ($\sim 5 \times 10^{17}$ cm^{-3} so that its resistivity does not differ greatly from that of the substrate. On top of this isolation, or intermediate, layer, the active epitaxial layer, with a concentration of $\sim 1 \times 10^{16}$ cm^{-3}, is grown. It is evident from the figure that the substrate defects do not propagate into the intermediate layer, and the active region is grown on an epitaxial layer with excellent crystal quality. This is, in effect, a method of growing a "substrate" crystal epitaxially. In fact, some structures were grown with sufficiently thick ($\sim$ 25 μm) intermediate layers to permit complete removal of the original substrate crystal during processing, thus producing an all-epitaxial device structure. The yield of epitaxial slices producing good breakdown characteristics increased dramatically when intermediate epitaxial layers were added.

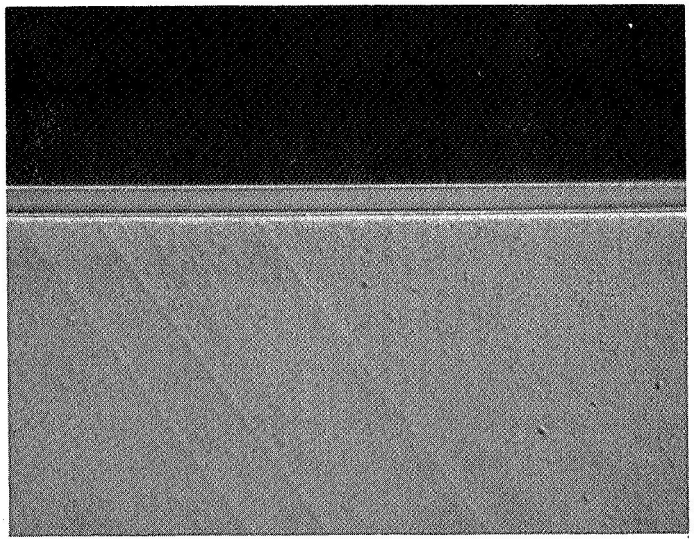

X 620

6915-2

Figure 3 Cleaved and Etched Cross Section of GaAs Epitaxial Slice for IMPATT Diode Fabrication

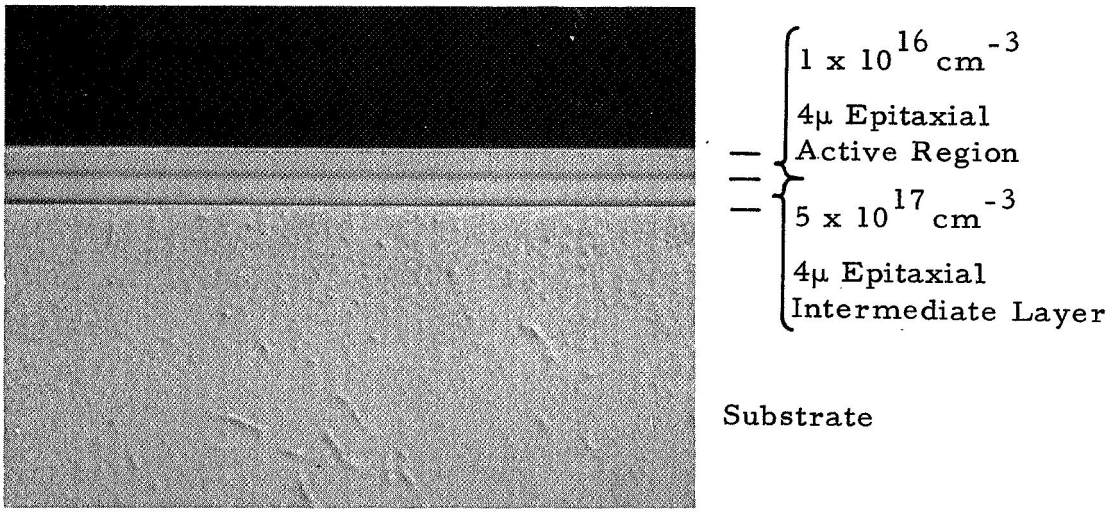

6915-3

Figure 4 Cleaved and Etched Cross Section of a Two-Layer GaAs Epitaxial Slice for IMPATT Diode Fabrication

C. Device Fabrication

The structure of the GaAs IMPATT diodes we have fabricated for microstrip operation has undergone several significant changes during the course of our development program. These changes were generally brought about because we felt that the device performance level could not be improved without changing the structure, or because it was difficult to reproduce results with a particular fabrication procedure. We have now arrived at a structure which can be reproducibly fabricated in a relatively straightforward fashion and which does not have the problems which caused inferior microwave performance at earlier stages in the program.

The present device structure is shown in Figure 5, along with its approximate dimensions. The structure has several critical features, which are discussed in detail below.

(1) Schottky Barrier Contact

We have used a number of different metals to make Schottky barrier contacts with volt-current characteristics suitable for IMPATT operation. The metals can be deposited by evaporation, sputtering, or plating. Plated platinum has been most successful, since it exhibits excellent adherence to the GaAs, is highly etch resistant, and provides uniformly good volt-current characteristics.

(2) n-Layer Properties

For X-band IMPATT operation, we have fabricated the most efficient diodes from n-GaAs with reverse breakdown voltages from 45 to 65 V. This range corresponds to doping levels in the n-layer from 1 to 2 x 10^{16} cm^{-3}. The corresponding depletion depths at reverse breakdown range from 2 to 3 μm. We have used n-layers from 4 to 6 μm thick, since this leads to high efficiency IMPATT operation without excessive susceptibility to failure modes caused by punch-through prior to reverse breakdown. Thinner n-layers (2 to 3 μm) would be required for TRAPATT operation, and tuning failures would be more likely to occur.

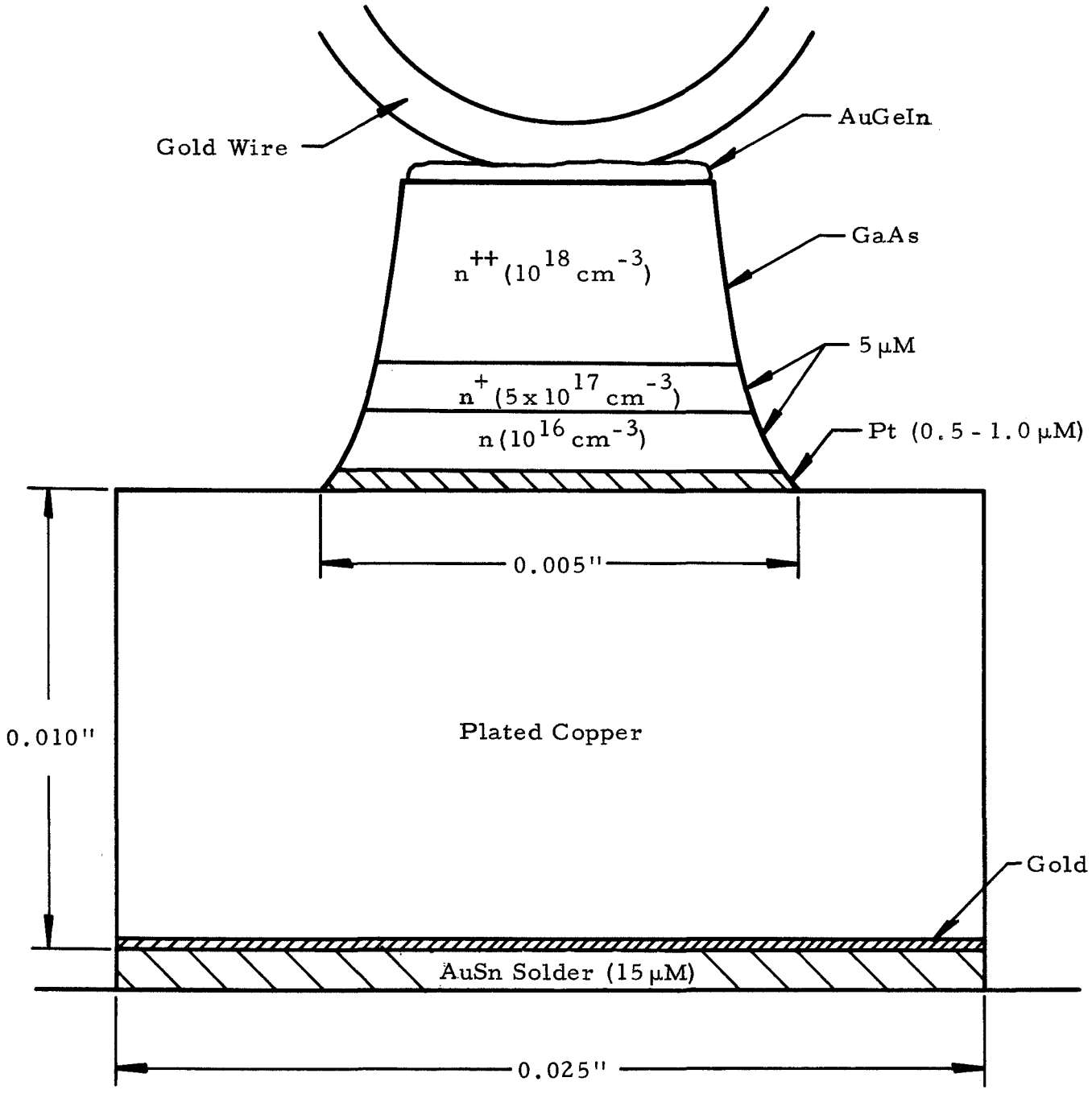

Figure 5 GaAs Schottky Barrier IMPATT Diode

(3) Intermediate n^+ Layer

An intermediate n^+-epitaxial layer between the active n-layer and the substrate eliminates many of the problems associated with substrate imperfections. A marked increase in the yield of good slices occurred after we incorporated this layer. Its presence may make TRAPATT operation possible for GaAs avalanche diodes.

(4) Ohmic Contact to the n^{++} Substrate

A $Au_{0.80}Ge_{0.10}In_{0.10}$ contact which alloys at $\sim 325°C$ was used in this program. A 0.001 inch Au wire is thermocompression bonded to the contact. We have found that an incompletely alloyed substrate contact acts as a resistance in series with the diode negative resistance and results in lower efficiency rf performance. (For a sufficiently poor contact, no microwave power is generated.)

(5) Mesa Diameter

The diode area for optimum X-band operation is 1 to 2 x 10^{-4} cm^2, corresponding to diameters of 0.005 to 0.006 inch. The zero bias capacitances of the diodes are 3.5 to 5.5 pF.

(6) Plated Copper Heat Sink

One of the most critical requirements for high power device operation is that provision must be made for rapid heat removal. In the case of an IMPATT diode, most of the heat is generated within 1 to 2 μm of the Schottky barrier contact, so that it is essential for this junction to be bonded to a good heat sink. This can be achieved most easily by plating a large area heat sink directly onto the device and then attaching the plated heat sink to a still larger heat sink. We use a plated copper heat sink with gold plated on the bottom. Copper has excellent thermal properties, and this procedure has enabled us to use high input powers in our devices.

Figure 6 outlines the fabrication steps used to obtain the diodes as shown in Figure 5. After appropriate cleanups, the platinum Schottky barrier

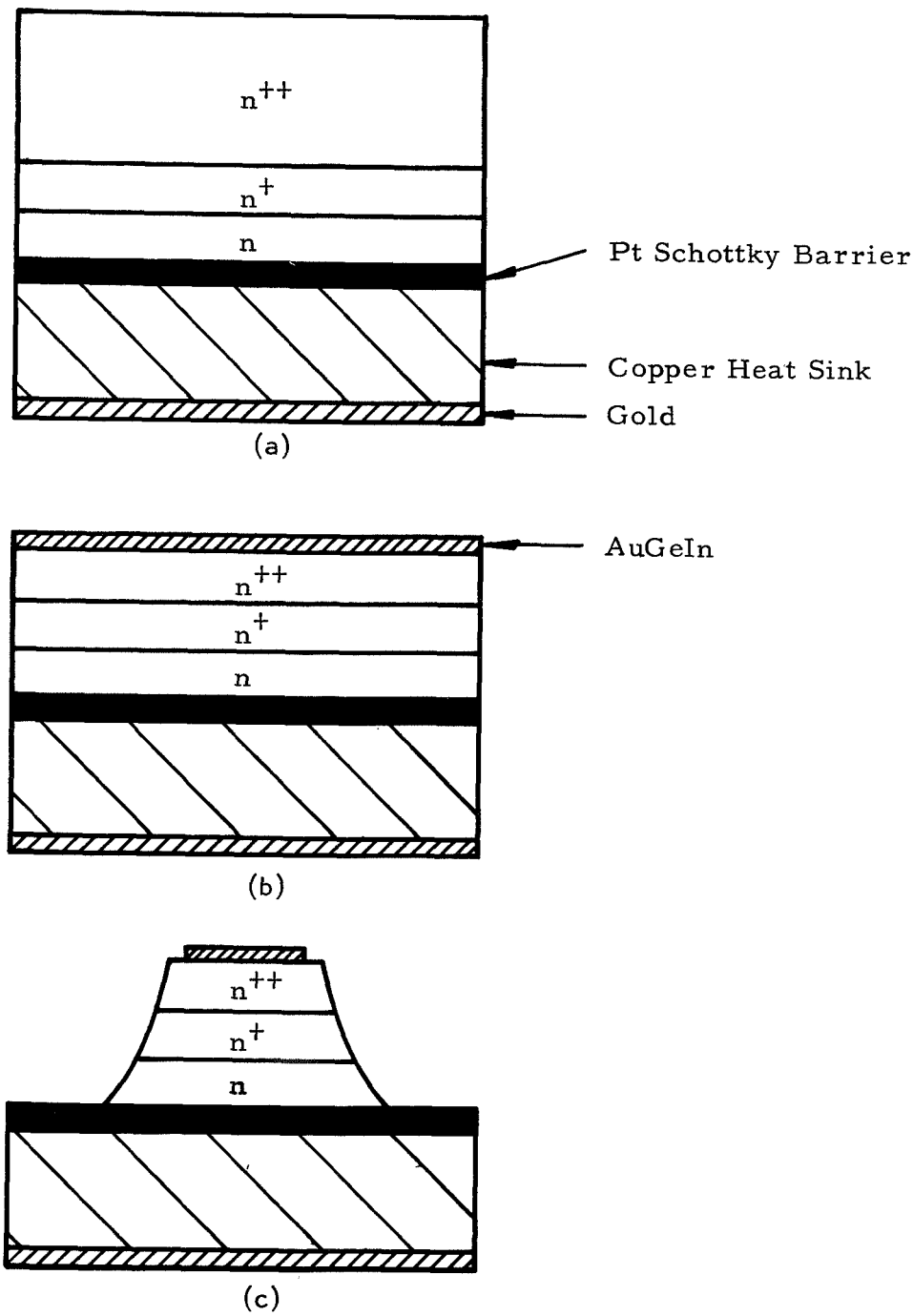

Figure 6 Fabrication Steps. (a) Plating, (b) thin substrate and contact, and (c) etch mesas.

is plated onto the n-layer, then a thick Cu plate, and finally a Au plate. Now, using the thick Cu as a support for the GaAs, we thin the GaAs to ~ 0.001 inch by lapping, etching, or a combination of the two. We then evaporate the AuGeIn contact. A circular dot pattern is defined by a photoresist process on the GaAs, and the mesas are then etched. Finally, the copper is cut or etched so that 0.025 inch square copper dies remain, with centered GaAs mesas.

D. Device and Material Evaluation

As an aid to the device fabrication phase of this program, it was important to develop means of evaluating our devices to identify the causes of device failure or poor microwave performance. At the beginning of the program, it was sometimes difficult to separate fabrication problems from materials problems, because good material is required to evaluate fabrication procedures, and good material can be recognized only if sound fabrication techniques are used. Very early in our work we identified a very large slice of good material (12179-122A) which we were able to use to develop our fabrication procedures. When these procedures became established, we were able with some confidence to evaluate other slices of material as they were processed.

The tests used in our device and materials evaluation are discussed in the subsections which follow.

1. Current-Voltage Characteristics

The I-V characteristics of the diodes are checked at various stages in the fabrication process, beginning immediately after the mesas are etched. Both the reverse and the forward characteristics are measured. A reverse I-V for a good microwave diode is shown in Figure 7(a). The device must have a very sharp reverse breakdown if it is to be capable of high efficiency microwave operation. However, the presence of a sharp break does not ensure good rf performance, since several other criteria must be met as well. A diode which exhibits a microplasma in its I-V curve is illustrated in Figure 7(b).

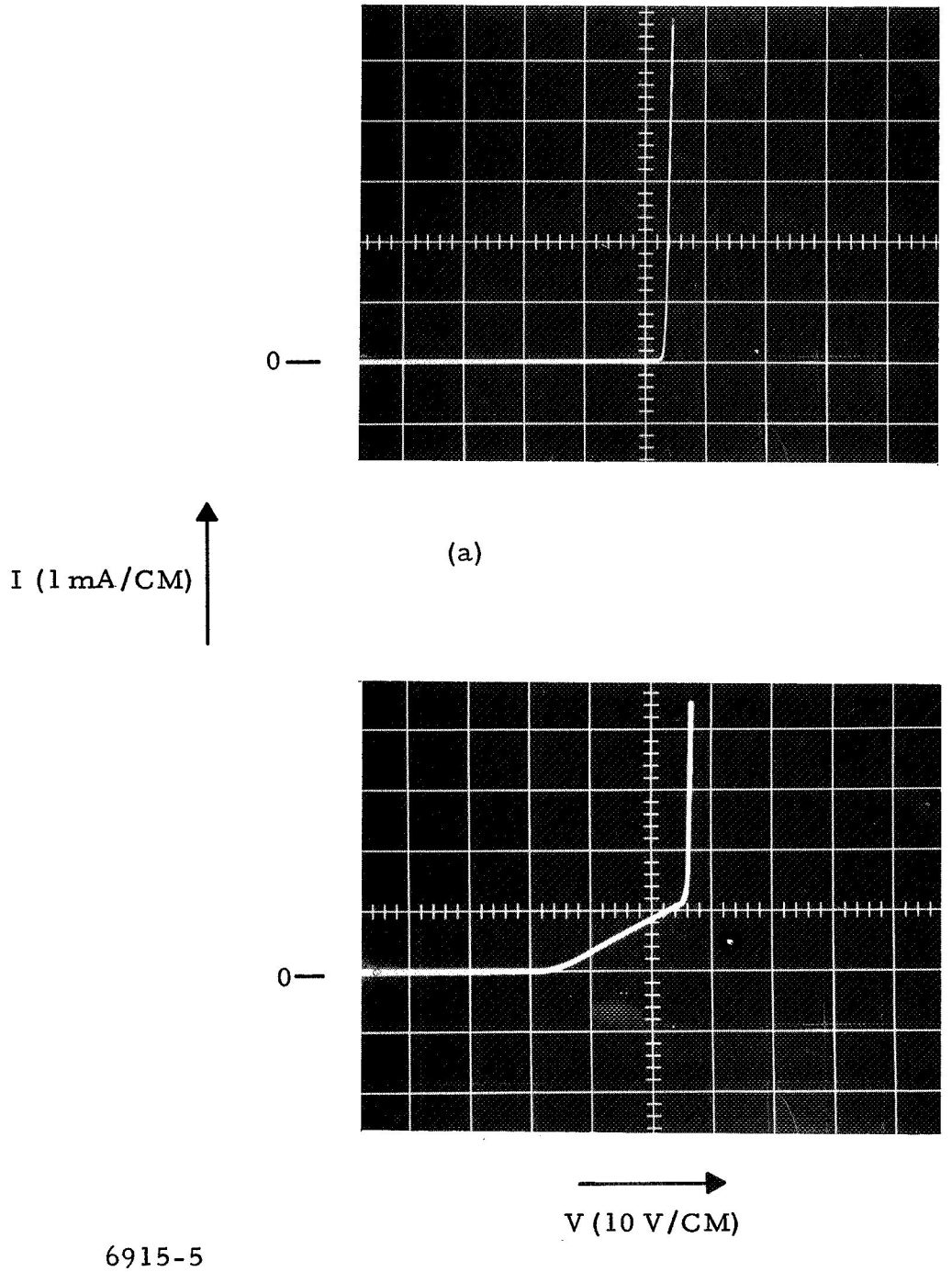

Figure 7 Reverse I-V Characteristics. (a) Good Schottky barrier, (b) microplasma.

There are several possible causes for the premature break at the lower voltage. Frequently, this behavior is due to microcracks. We have incorporated changes in our fabrication procedures to eliminate this type of problem.

It is also essential to check the forward I-V of these diodes, particularly at high current levels. We can determine from the slope of the curve whether or not there is a significant resistance in series with the diode. Figure 8 shows the forward I-V for two diodes. Curve (a) is the curve for a good diode with low series resistance, while curve (b) is for a diode with sufficient series resistance to reduce its efficiency significantly.

2. Doping Profile

An automatic impurity profile plotter which utilizes the differential capacitance technique has been used to evaluate the quality of the epitaxial material before a slice is processed. Figure 9(a) shows a typical doping profile for a good material, yielding about 10% efficiency and 700 to 900 mW in X-band. The doping profile is not necessarily flat for efficient operation of the diode. Normally, the doping density varies as $x^{[(1/n)-2]}$ for an epitaxially grown material; x is the distance from the Schottky barrier contact into the epi-layer, and n varies from 1/2 for a flat doping profile to 1/3 for a linearly increasing impurity density. The impurity plotter is also capable of detecting a high resistivity layer existing between the n active layer and the n^+ substrate. Figure 9(b) shows an example of such a layer. This high resistivity "notch" is not desirable because it is in series with the microwave negative resistance of the diode and would reduce the conversion efficiency of the diode drastically. Good correlation has been obtained between the results of the doping profile measurements and the microwave performance results.

3. Thermal Resistance Measurements

There are two main contributions to the thermal resistance, r, of an IMPATT diode. The first is a laminar flow term which accounts for the heat flow within the active region and the contact metallization (see Figure 5).

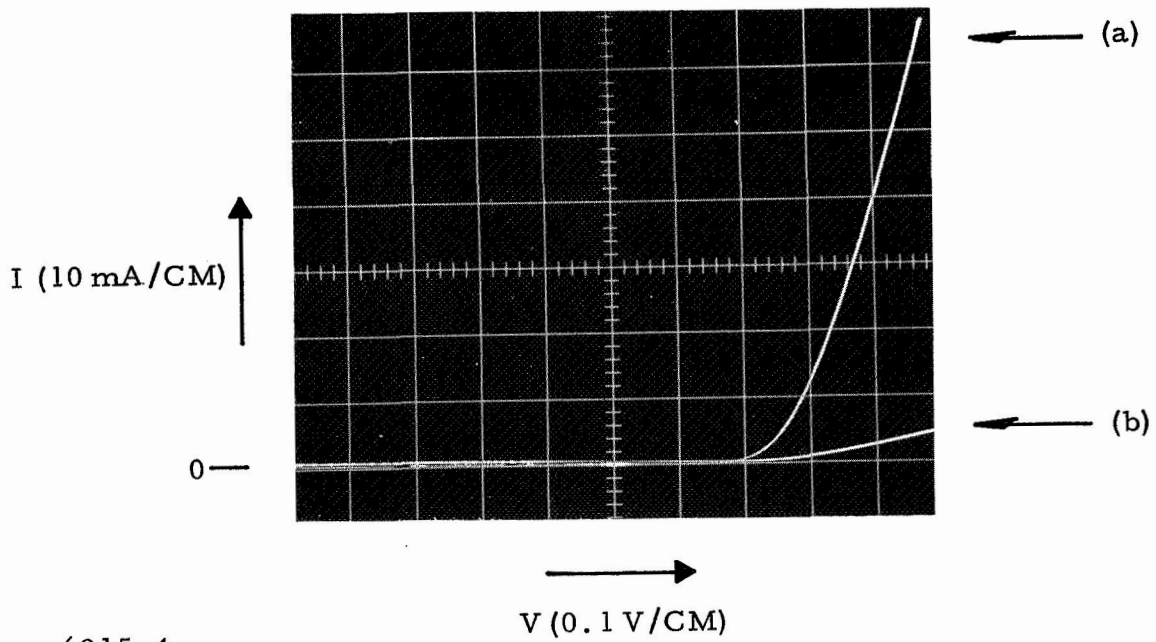

Figure 8 Forward I-V Characteristics. (a) Low series resistance curve, (b) high series resistance curve.

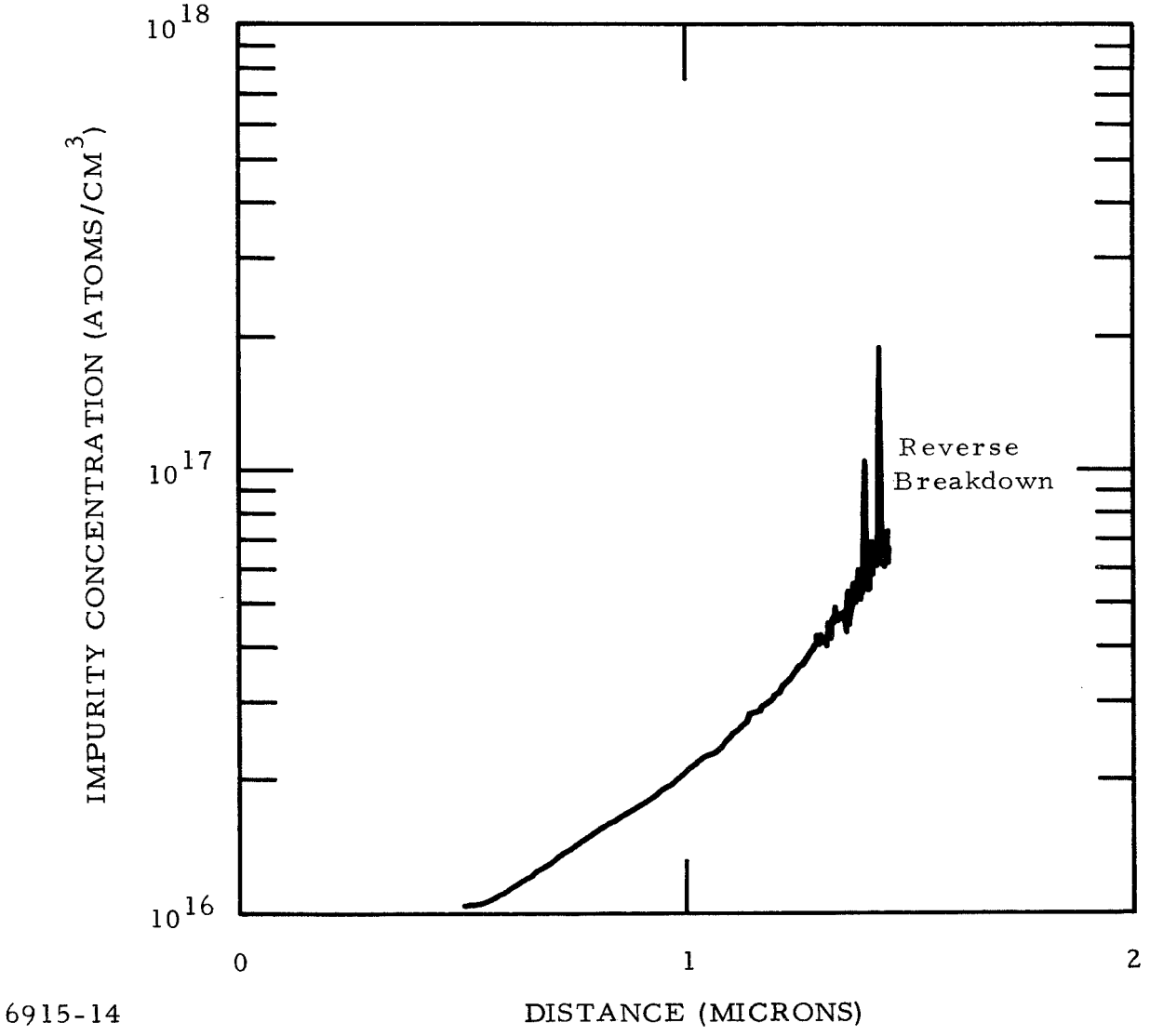

Figure 9(a) Impurity Profile of a Good Slice

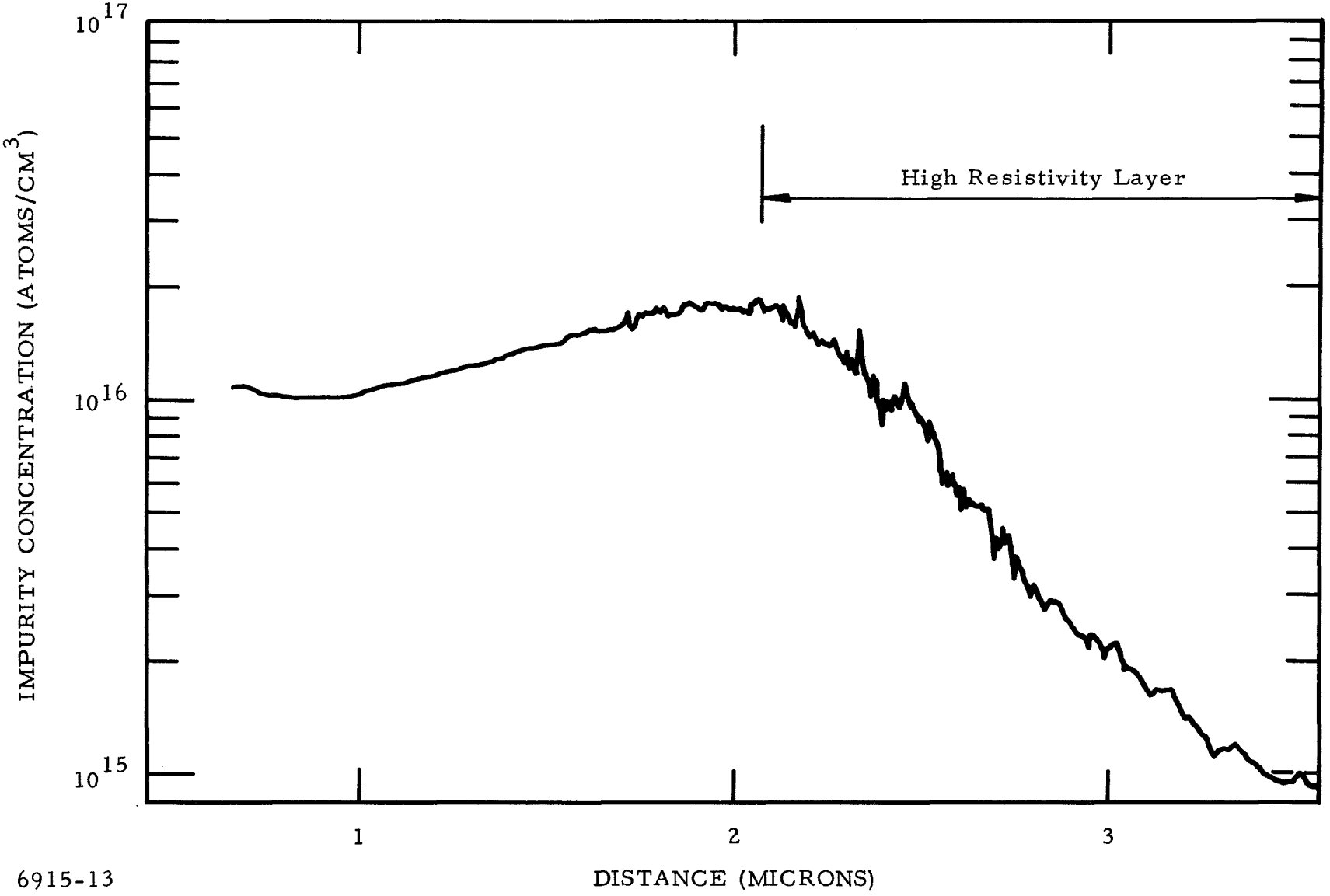

Figure 9(b) Impurity Profile of a Slice with High Resistivity Layer

The second, and most important, contribution is a term due to the hemispherical spreading of the heat into the copper.

We have developed a method of determining this thermal resistance in avalanche devices by measuring the I-V characteristic. Figure 1(a) shows a sketch of the I-V characteristic of an avalanche diode. The breakdown voltage V_B is a function of temperature (via the temperature dependence of the ionization coefficients). The incremental resistance at the operating point can be written

$$R_S = R_{SC} + R_{TH} \quad , \tag{1}$$

where R_{SC} is the space charge resistance and R_{TH} is the resistance (electrical) due to thermal effects. The space charge resistance is given by

$$R_{SC} = \frac{W_D^2}{2\epsilon v_d A} \quad , \tag{2}$$

where W_D is the length of the drift region, ϵ is the dielectric constant, v_d is the saturated carrier velocity, and A is the junction area. R_{SC} is frequency independent up to the transit time frequency of order v_d/W. The thermal component of the electrical resistance R_{TH} has been shown by Haitz, et al.,[5] to be related to the thermal resistance r by

$$r = \frac{R_{TH}}{\beta V_B^2} \quad , \tag{3}$$

where β is the temperature coefficient of the breakdown voltage given by

$$\beta = \frac{\partial}{\partial T} (\log V_B) \quad . \tag{4}$$

We have measured β for GaAs IMPATT diodes to be 1.4×10^{-3} °C^{-1}. Since R_{TH} is strongly frequency dependent (falling to $\sim$ 3% of its dc value at 1 MHz), R_{TH} can be determined by measuring R_S at low and high frequencies.

This reverse bias method for obtaining thermal impedance values has the advantage of being an in situ method, in contrast to previous forward-bias pulse techniques, and allows evaluation of the heat sink structure mounted in the electronic circuit of interest.

4. Evaluation of Microwave Performance

Coaxial cavity and waveguide circuits have been used to evaluate the microwave performance of IMPATT diodes mounted in varactor packages.

Figure 10 shows a coaxial cavity capable of matching diode impedance over wide frequency ranges. The double-slug quarter-wave transformer with variable characteristic impedance is used to tune the diode. The slugs are adjusted until maximum power and a single frequency are obtained. Experimentally, it has been found that one of the slugs should be placed near the device to form a resonant cavity, while the other slug provides fine tuning. Because of the high input power density required, a special heat sinking arrangement is designed. This circuit has been used effectively for C- and X-band to test diodes with differing areas and breakdown voltages. However, since the tuning associated with this circuit is abrupt, some diodes failed while the slugs were being adjusted for maximum output power. Although the exact cause of "tuning failures" has not yet been determined, these failures could be caused by transient redistribution of the current density, which is higher along the diode edges because of the temperature dependence of the breakdown voltage and the fact that the temperature of the center of the mesa is normally higher than that of the edges. The failures caused by tuning have usually occurred along the edges. To circumvent this problem, an X-band waveguide test circuit, shown in Figure 11, has been used. It consists of a diode mount, a sliding short, and a slide screw tuner. Since the negative resistance of the diode is normally of the order of a few ohms, an impedance-matching metallic "hat" is needed to obtain maximum power. The optimum size of the hat to be used for maximum power depends on the breakdown voltage of the material and the area of the diode. For X-band diodes with areas of $\sim 10^{-4}$ cm^2

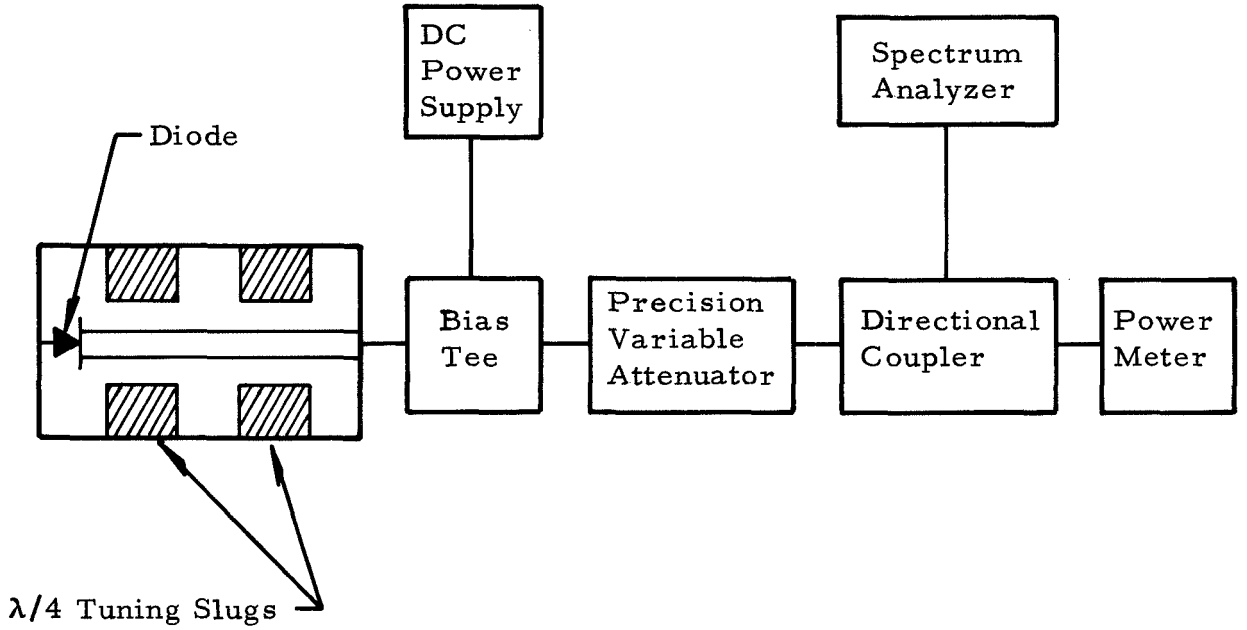

Figure 10 Coaxial Cavity Circuit

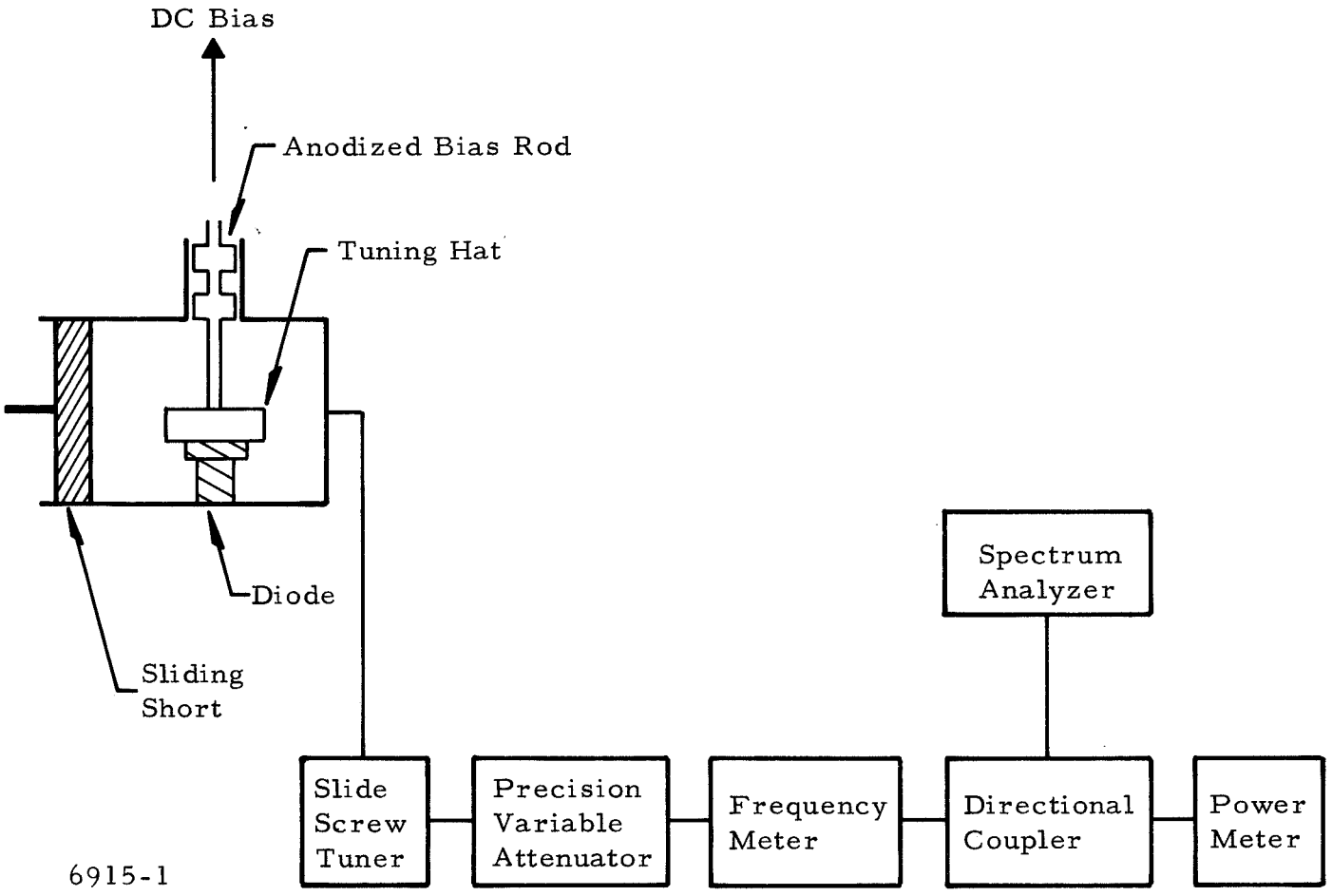

Figure 11 X-Band Waveguide Circuit

(zero bias junction capacitance of 3 to 5 pF) and breakdown voltages of ~ 50 volts, it has been found that the same metallic hat can be used. In general, the smaller the hat, the higher the oscillation frequency. To avoid "tuning failure," the input power is increased in small steps, and at each power level the slide screw tuner and sliding short are adjusted accordingly for maximum rf output. Normally, only a minor adjustment of the sliding short and slide screw tuner is necessary. Prior to device failure, multifrequency output can generally be seen on the spectrum analyzer. This could be due to development of a weak spot, causing the rf output to be incoherent. Figure 12 shows the microwave performance of a 1 watt, 14% efficiency X-band diode tested in the waveguide circuit. Table I summarizes the best results obtained from each slice for which microwave oscillations were observed. A large number of slices for which no oscillations were observed were processed prior to the introduction of the n^+ intermediate layer. Almost all the slices processed with an intermediate layer have exhibited oscillations, but some were much more efficient than others.

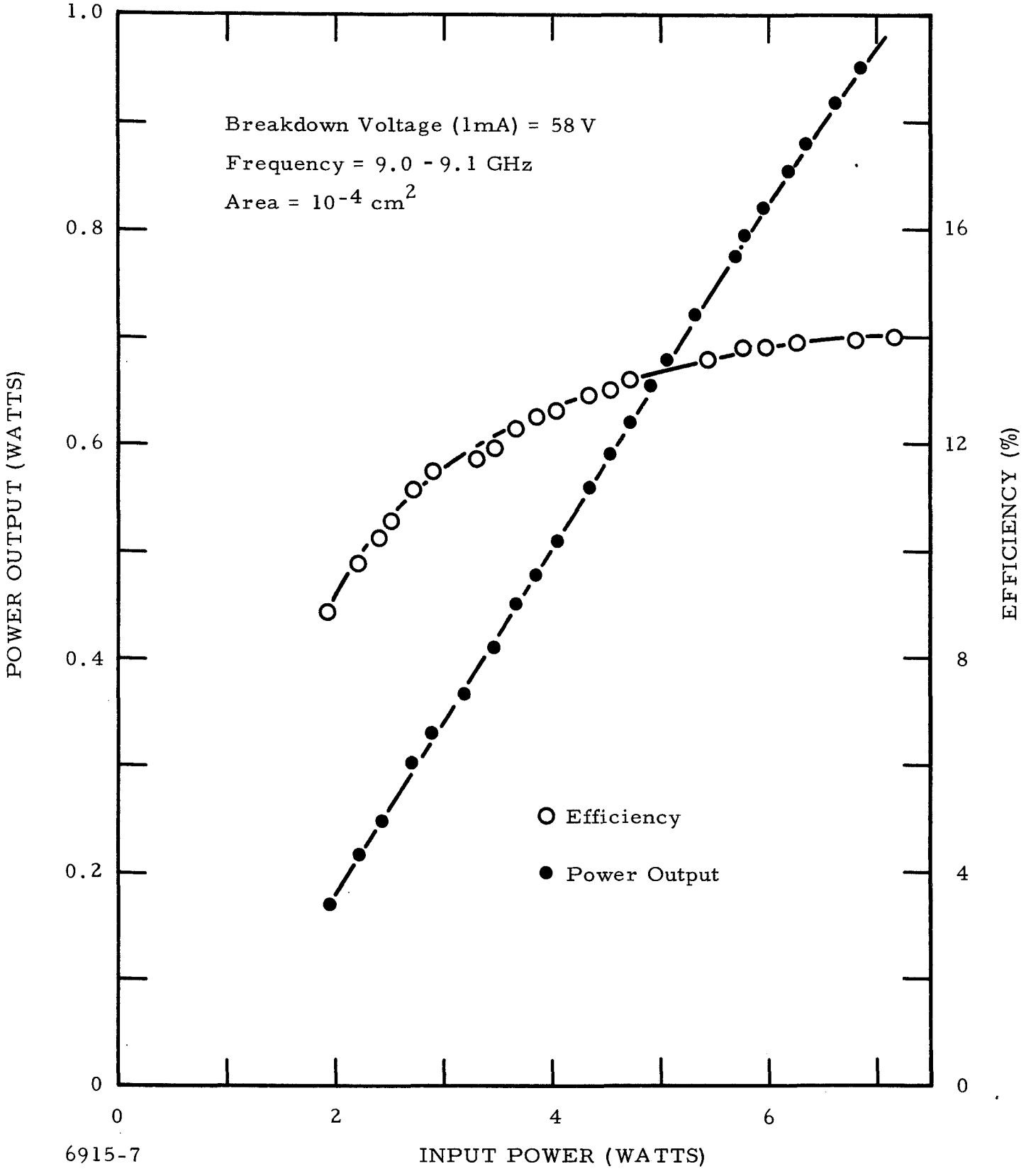

Figure 12 rf Power and Efficiency vs Input Power

Table I

GaAs IMPATT RESULTS

SLICE NUMBER	n(μm)	n^+(μm)	V_{rb}(V)	SCHOTTKY METALS	P_{in}(W)	f(GHz)	P_{rf}(mW)	η(%)
12179-122A	4-5	---	44	Ni-Au	10.3	7.8	263	2.6
			40	Mo-Au	9.1	9.6	562	6.2
			38	Pt-Mo-Au	10.3	10.2	750	7.3
-132A	5.5	---	66	Mo-Au	4.3	8.9	170	3.9
-123	6	---	48	Pt-Mo-Au	2.9	9.25	185	6.4
-110	6	---	42	Pt-Mo-Au	4.7	10.2	142	3.0
12526-61B	5	---	45	Pt plate	5.48	9.8	410	7.5
-68	6	---	46	Pt plate	7.7	8.8	160	2.07
-61A	6	---	60	Pt plate	3.64	8.8	130	3.57
12875-32	4.5	5	59	Pt plate	6.27	8.9	680	10.7
-33	3	4.5	59	Pt plate	5.54	8.2	255	4.60
-35	6	5.5	52	Pt plate	9.0	9.0	900	10.0
-42	6	4.5	48	Pt plate	7.07	9.1	720	10.20
-64	10	4.3	52	Pt plate	4.35	9.75	175	4.02
-66	6	6-7	57	Pt plate	4.69	9.4	450	9.6
-67A	6	3	60	Pt plate	5.80	9.04	740	12.7
-67B	6	3	60	Pt plate	6.76	8.9	720	10.6
-69A	7.2	4.3	55	Pt plate	6.90	8.75	680	9.84
-69B	5.8	4.3	58	Pt plate	7.15	9.1	1000	14.0
-71	6	6	55	Pt plate	6.86	9.2	965	14.1
-72A	6	7	58	Pt plate	4.1	8.9	200	4.9
-81	6	7.2	45	Pt plate	5.14	9.1	390	7.6
-40	7.5	5	60	Pt plate	9.83	9.0	1200	12.2

SECTION III

CIRCUIT DEVELOPMENT

A. Diode Characterization

Microwave impedance measurements of IMPATT diode junction parameters are important both for designing optimum circuits and for evaluating diode quality.[6] The laboratory setup used to measure diode impedance is shown in Figure 13. The diode is mounted as the termination of a 50-ohm coaxial line to suppress any oscillation when the diode is biased above avalanche breakdown. Because of the negative resistance available, the diode acts as a reflection amplifier. The VSWR's and the phase angle of the reflected wave can be measured by using the slotted line. A Smith chart can then be utilized in calculating the diode impedance at the junction. We have found that a calibration procedure is necessary. Figure 14(a) shows a complete equivalent circuit of a diode in a varactor package. The parasitic elements include package capacitance C_{PK}; wire inductance L_w; fringing capacitance C_F; series resistance R_S, contributed by the unswept epitaxial region; and contact and spreading resistances. The parameters to be measured are junction capacitance C_J, avalanche inductance L_D, and negative conductance G_D due to the avalanche and transit time effects. Below avalanche breakdown, $G_D = 0$ and $L_D = \infty$, so that the equivalent circuit can be represented by the circuit shown in Figure 14(b). The network between the measurement plane and the diode junction can be changed to an ideal transformer with turn ratio N plus the network reactance X and equivalent series resistance R_S'. Writing the measured impedance at the measurement plane as $R_m + jX_m$, we have

$$R_m + jX_m = N^2\left[R_S' + j\left(X - \frac{1}{\omega C_J}\right)\right] \quad . \tag{5}$$

Equating the imaginary part of both sides of Equation (5), we obtain

$$X_m = N^2 X - \frac{N^2}{\omega C_J} \quad , \tag{6}$$

where C_J is the low frequency ($\sim$ 100 kHz) capacitance measured by a conventional capacitance bridge. Since C_J decreases as the reverse bias voltage is increased,

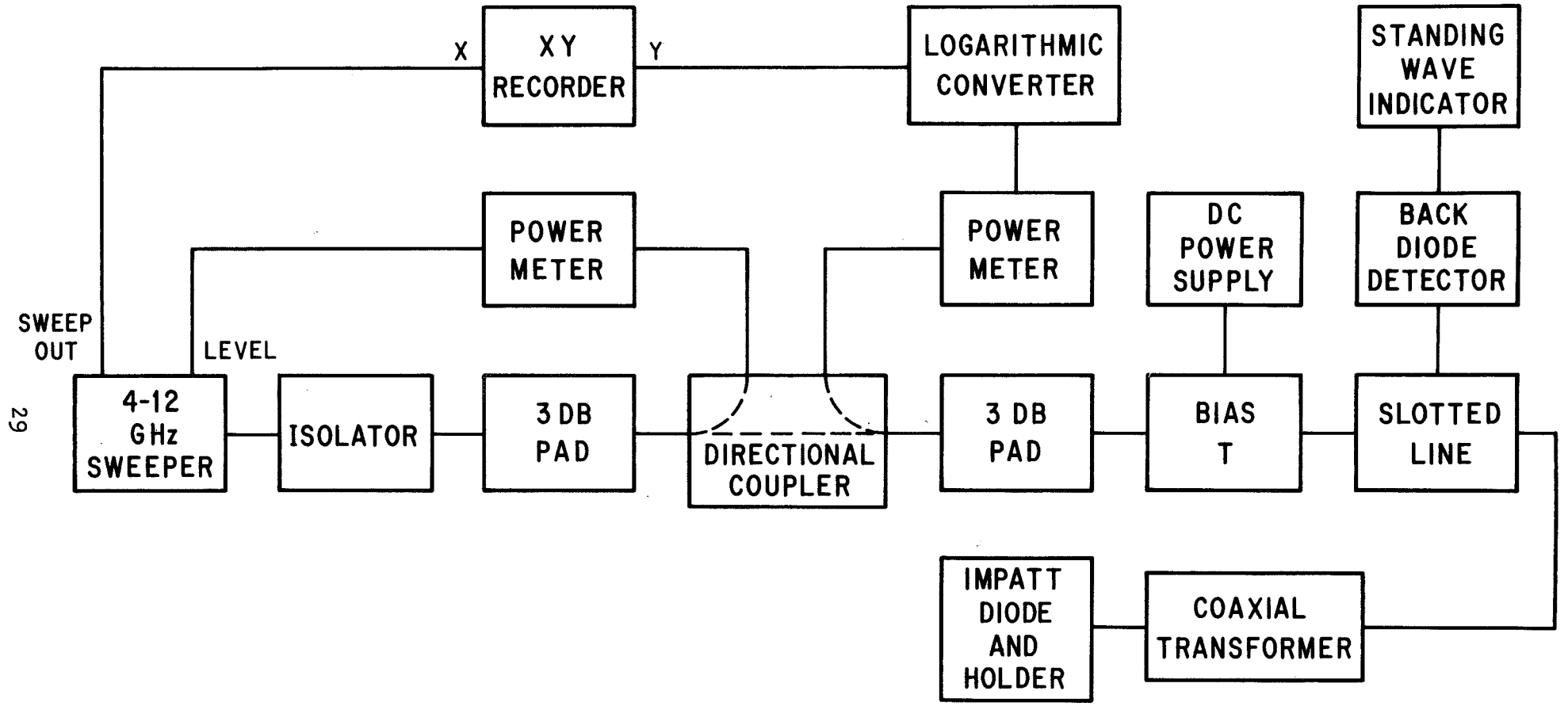

Figure 13 Characterization Set-Up

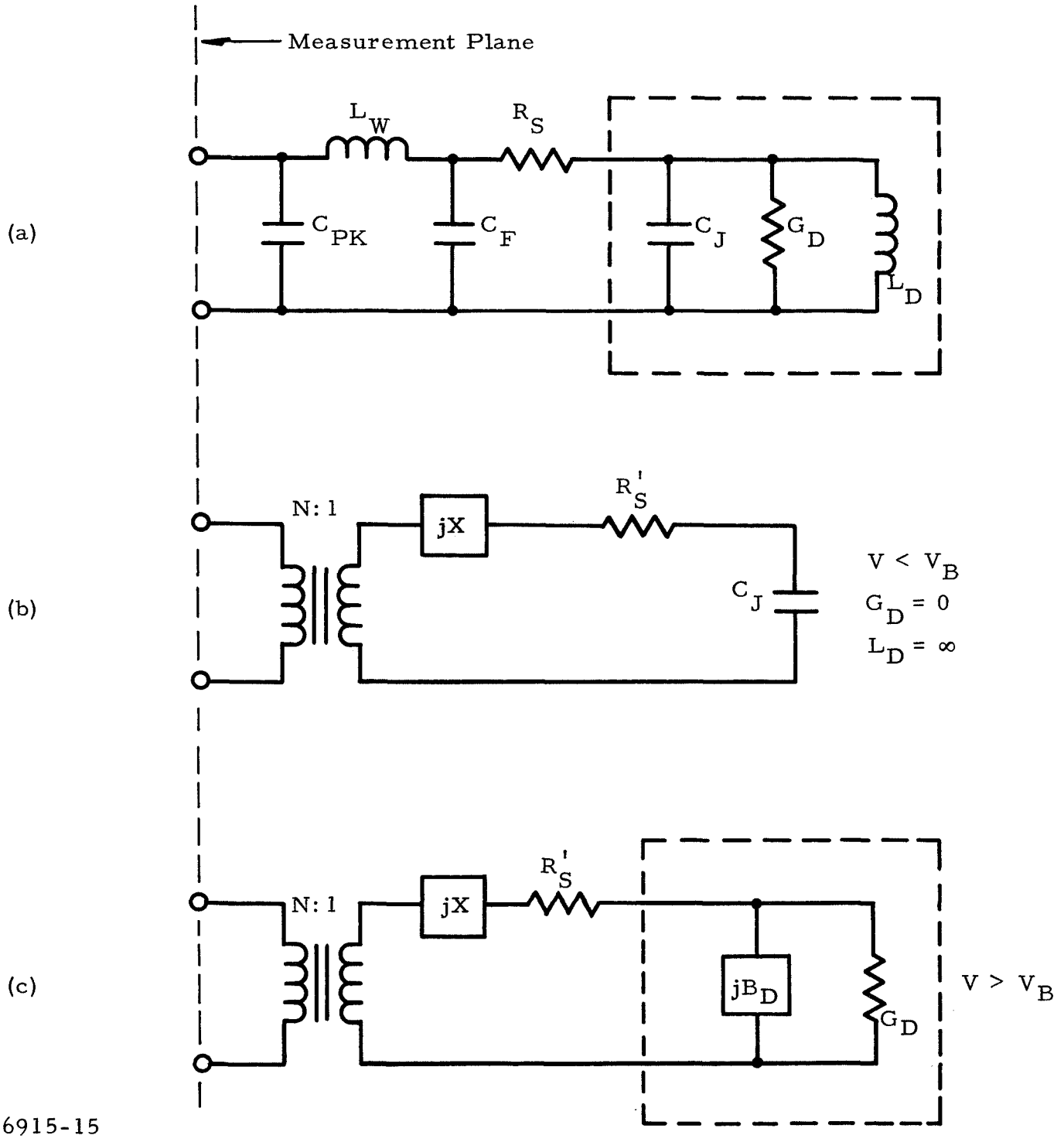

Figure 14(a) Packaged IMPATT Diode Equivalent Circuit
(b) Representation - Below Breakdown
(c) Representation - Above Breakdown

the turn ratio N and network reactance X can be determined from a plot of X_m vs $1/\omega C_J$ at different reverse bias voltages up to breakdown by using a digital computer. This is illustrated in Figure 15. It should be noted that the network parameters (N and X) are valid only at the measurement frequency. Once the network parameters are determined, the diode impedance, as indicated by $G_D + jB_D$ in Figure 14(c), can be measured as a function of rf voltage, current density, and frequency. A typical variation of the parasitic series resistance and capacitance with the reverse bias voltage is shown in Figures 16(a) and (b). Experimentally, we have found that the series resistance at breakdown R'_{BR} should be minimized to reduce the rf loss and, thus, increase the conversion efficiency. For efficient diode operation, R'_{BR} should be minimized to reduce the rf loss and, thus, increase the conversion efficiency. For efficient diode operation, R'_{BR} should be less than one ohm, since the negative resistance of the diode is only of the order of a few ohms at the optimum current density and frequency. The good agreement between the low frequency and microwave C-V data indicates that the network parameters thus obtained are reasonably accurate. Figure 17 shows a typical admittance plot of a GaAs diode fabricated in our laboratory. For an X-band diode with a breakdown voltage of 50 to 60 volts and current density of ~ 500 A/cm^2, the negative conductance is about 10^{-3} mho, while the susceptance is about 10^{-2} mho, resulting in a device negative Q of ~ 10. The following impedance behavior of the avalanche diode should be observed in an IMPATT oscillator or amplifier:

(1) The maximum negative conductance shifts to higher frequency as the breakdown voltage is lowered. This is due to the reduced drift region width, which results in a shorter transit time.

(2) The optimum frequency for maximum output power is about 1.5 times the avalanche frequency for a given current density.

(3) The negative conductance decreases as the rf voltage is increased, thus leading to a stable oscillation. This effect is due to the widening of the avalanche zone during the avalanching cycle and the reduction of the electric field below that required for velocity saturation in the drift region during the drift cycle. These two factors

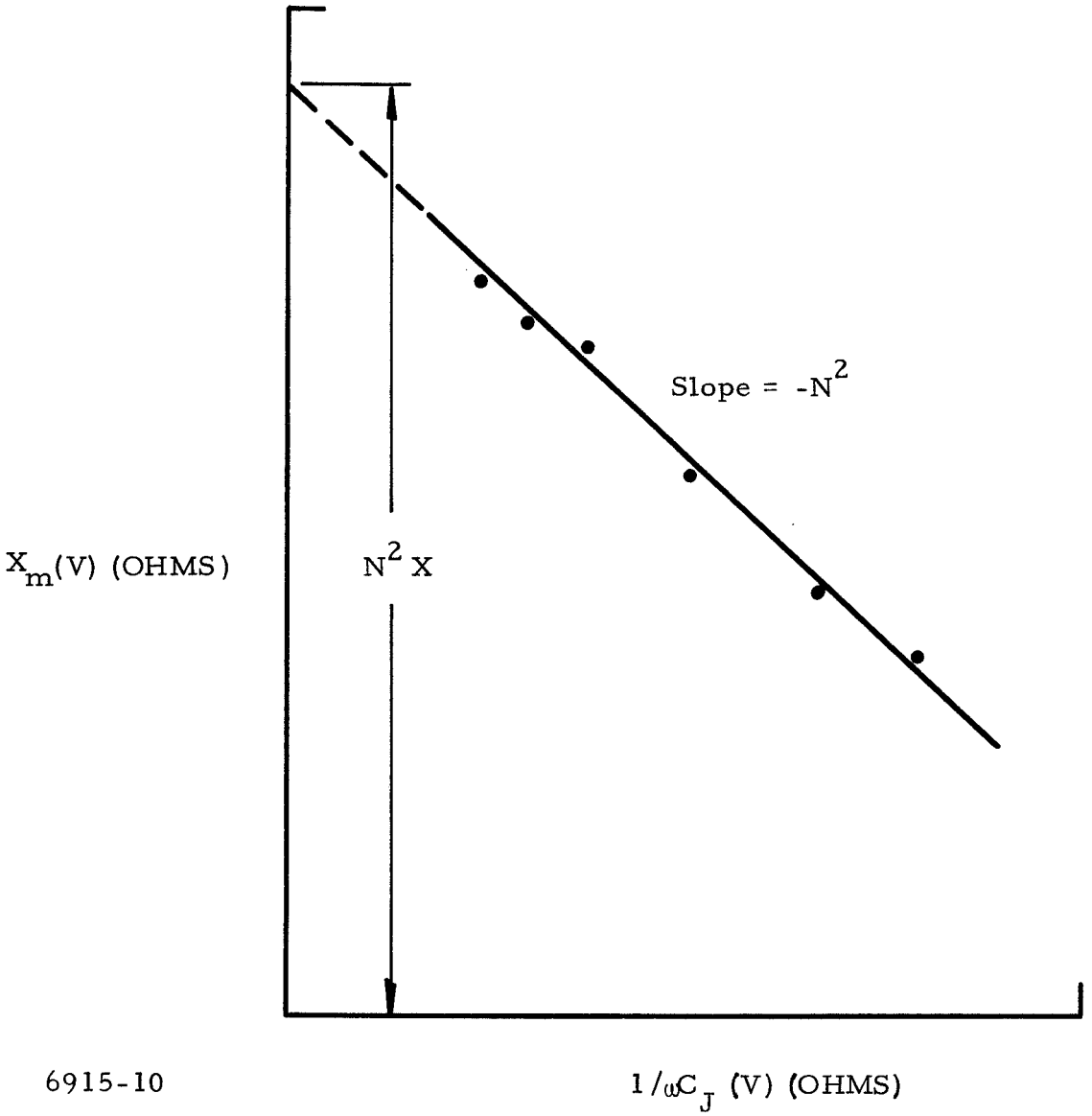

Figure 15 X_m vs $\frac{1}{\omega C_J}$

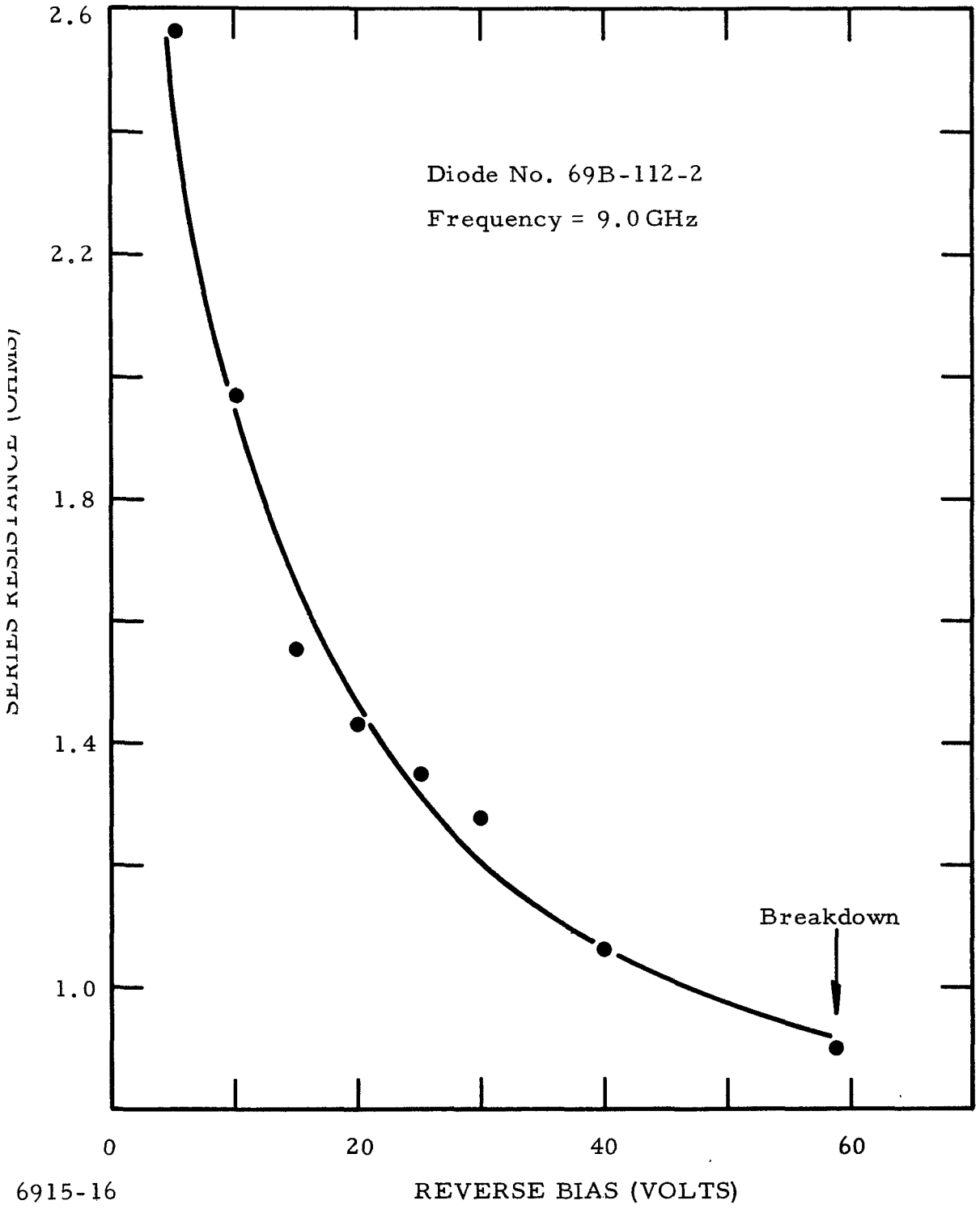

Figure 16(a) Series Resistance vs V

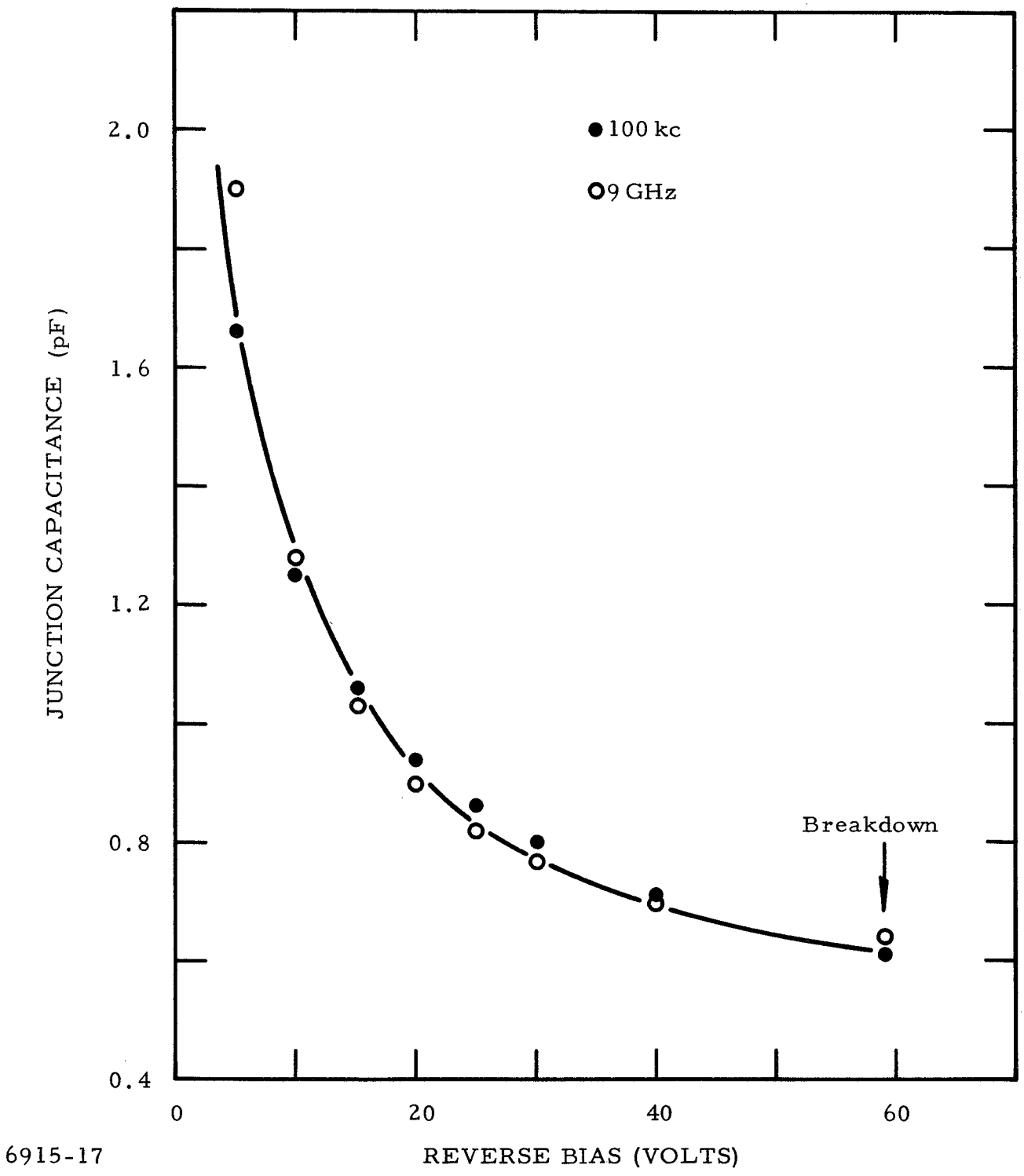

Figure 16(b) Junction Capacitance vs V

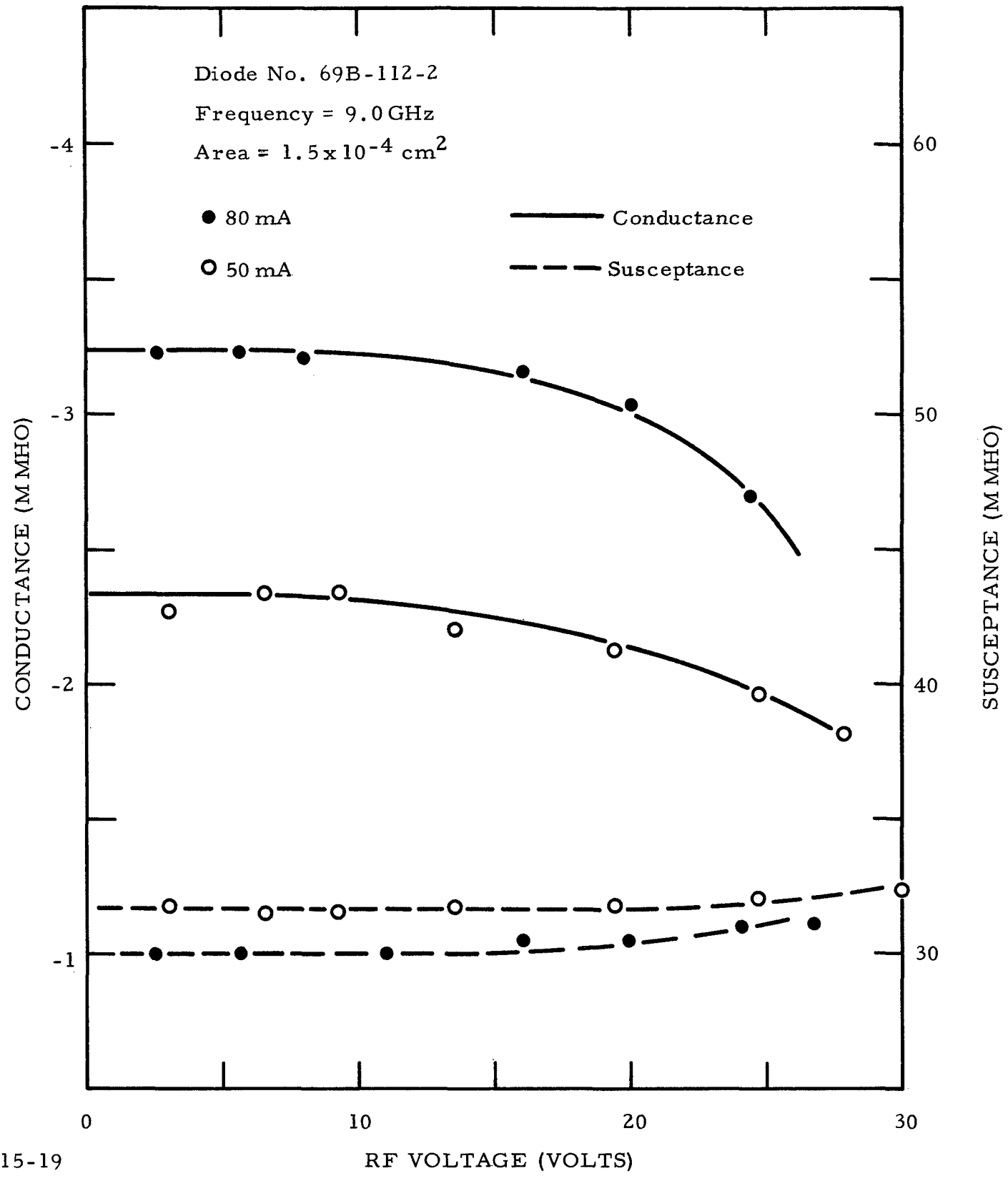

Figure 17 Admittance vs rf Voltage

reduce the phase angle between the rf voltage and current and result in power saturation. The dc input current also limits the amplitude of the rf current swing. The diode susceptance increases only slightly as rf voltage is increased. The equivalent series negative resistance also decreases as a function of increasing rf voltage, since the device susceptance is about one order of magnitude higher than the negative conductance.

(4) At a given frequency and rf voltage, the negative conductance increases while the susceptance decreases with the current density.

These general trends of the diode impedance behavior are helpful in designing a microstrip IMPATT oscillator or amplifier. The design and fabrication of an X-band microstrip GaAs IMPATT oscillator are described in Section III.B of this report.

B. Development of Microstrip IMPATT Oscillator

Figure 18 shows the microstrip circuit that has been used successfully in this work.[7] The oscillator circuit consists of a quarter-wave transformer and a 50-Ω output transmission line soldered to an OSM connector. The thin-film transmission line is fabricated by etching a Cr-Au film on a 10-mil thick alumina substrate. The dc bias is introduced through a bias pad to the lowest impedance point of the circuit. The device is soldered directly to a copper block attached to a heat sink. This heat sinking method provides a low thermal resistance. A series of microstrip circuits with different characteristic impedances for the quarter-wave transformers is fabricated to provide impedance matching for diodes fabricated from different slices with different breakdown voltages and doping profiles. In general, the negative resistance ranges from 3 to 10 ohms, while the capacitive reactance ranges from 20 to 40 ohms. Figure 19 shows the performance of a GaAs IMPATT oscillator in microstrip circuit. This oscillator delivers 810 mW rf power at 10.1 GHz and 11% efficiency. A diode with smaller area requires a higher circuit resistance for optimum matching. Because tuning adjustment is not possible in microstrip circuit, the frequency, bias level, impedance level, etc., should be considered when a microstrip oscillator is being designed. Our experience indicates that a good rf connection at the

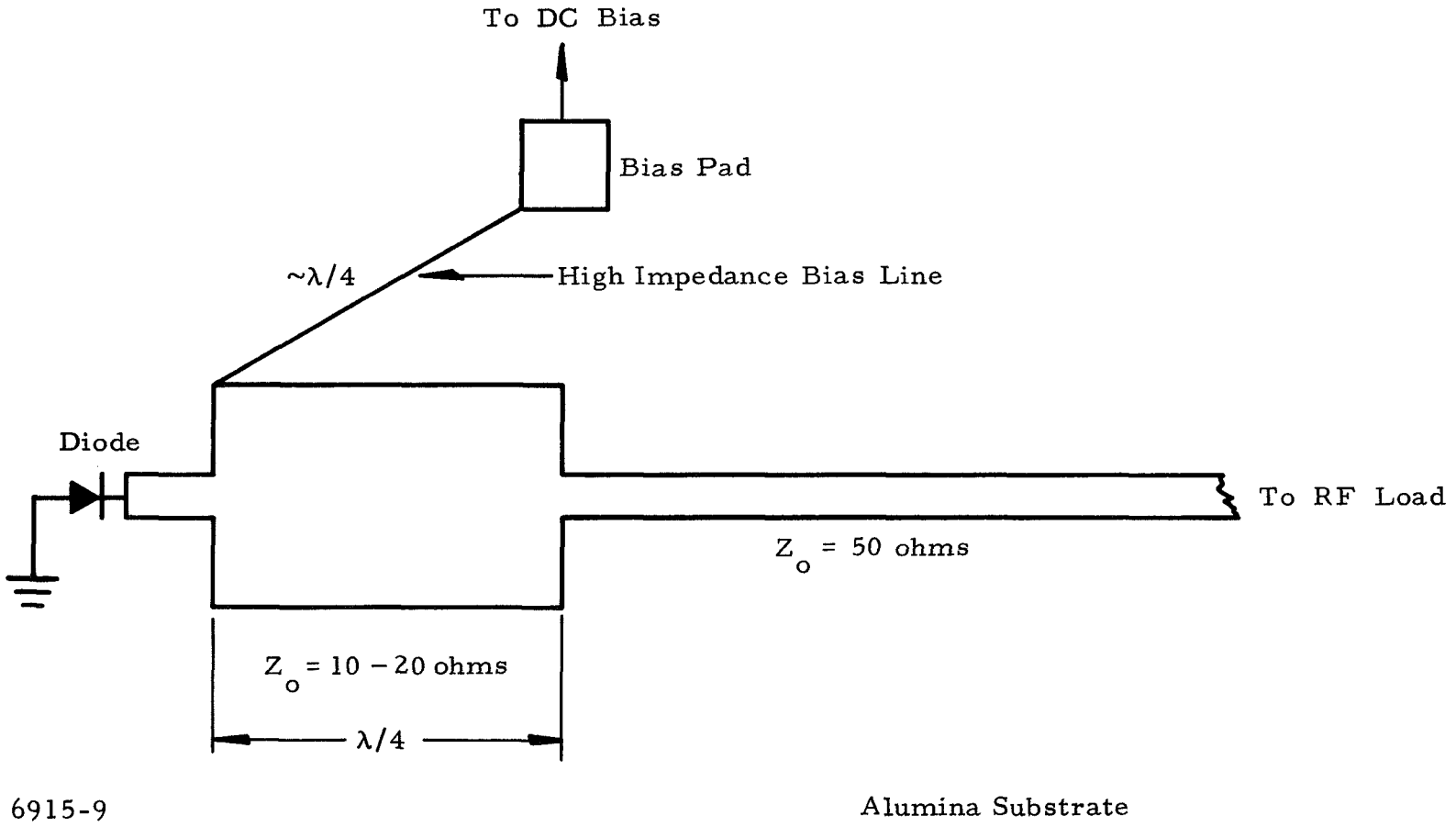

Figure 18 IMPATT Microstrip Circuit

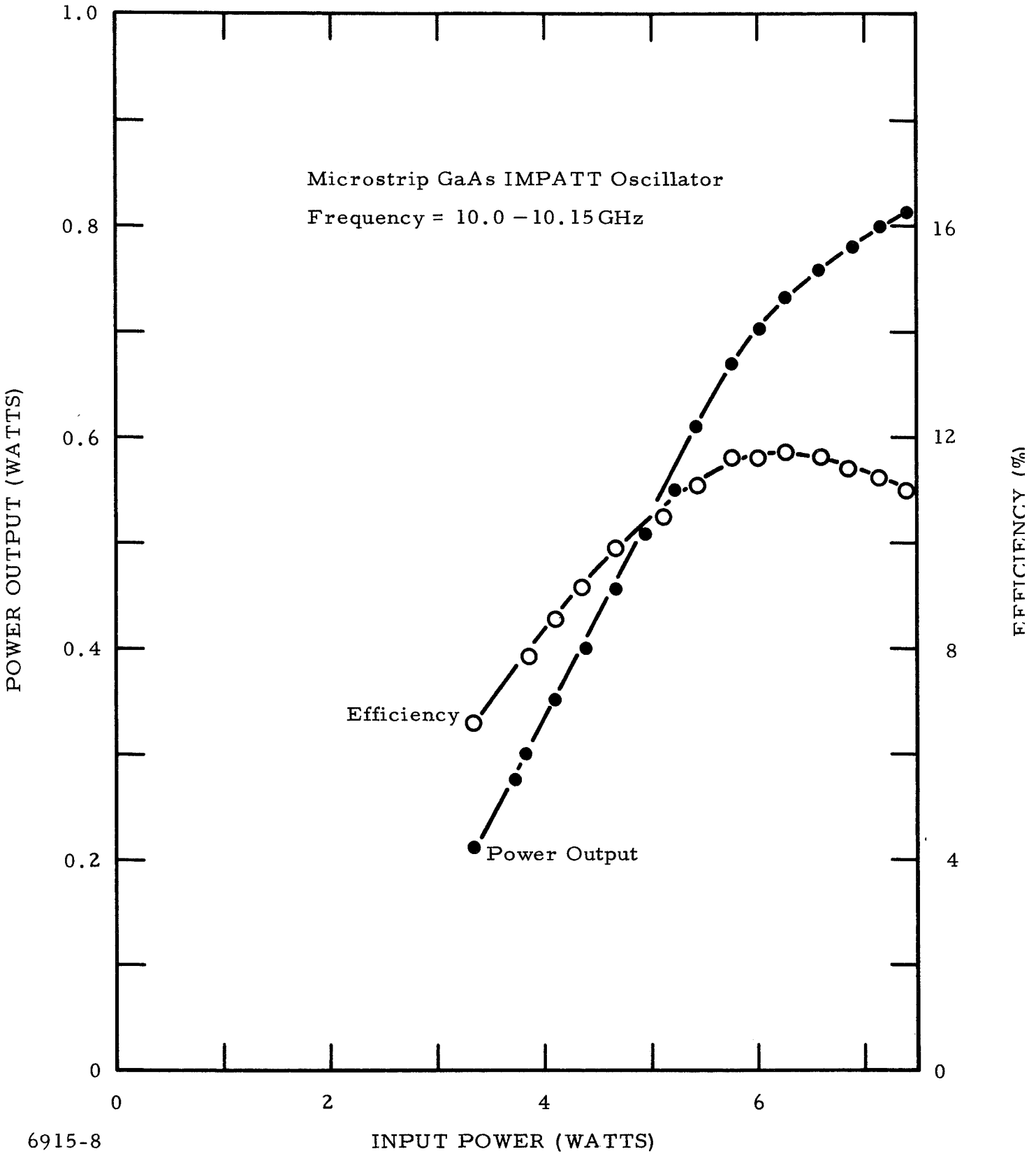

Figure 19 rf Performance in Microstrip

output of the 50-Ω strip line is very important for good rf performance. Photographs of the type of circuit which will be delivered to NASA are shown in Figure 20.

C. TRAPATT Requirements

Although the diodes produced thus far have not been capable of operating in the TRAPATT mode because the n epitaxial layer is too thick to permit punch-through, a microstrip circuit that can be used to operate the diode in the TRAPATT mode from C- to X-band is recommended. The circuit is shown in Figure 21. Basically, it consists of a resonant cavity at IMPATT frequency, a section of 50-Ω line about a half wavelength long at TRAPATT frequency, and a low pass filter to prevent higher harmonics of the TRAPATT frequency from coupling to the external load. The low pass filter is made up of multisections of impedance transformers. The characteristic impedances and positions of the tuning transformers are adjusted according to the type of diode and the desired frequency of operation. For TRAPATT operation at C-band, a diode designed for X- or K_u-band IMPATT operation would be required. Because of the more stringent circuit requirements, the design of a microstrip TRAPATT oscillator would be more critical than that of the IMPATT oscillator.

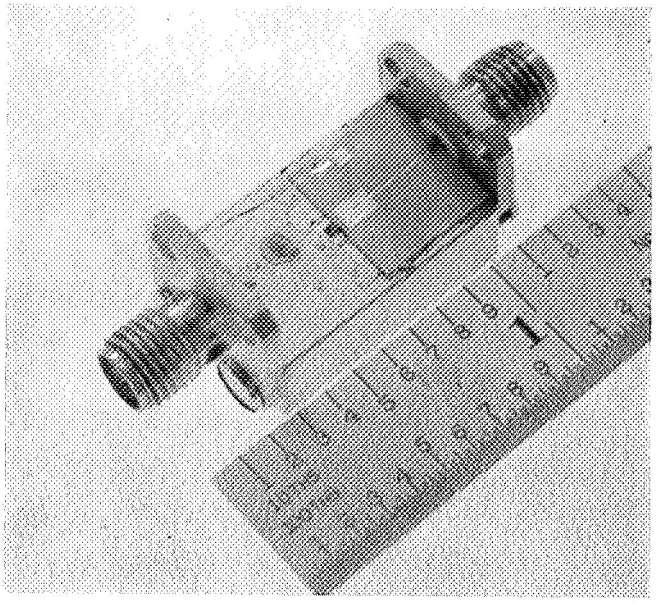

(a)

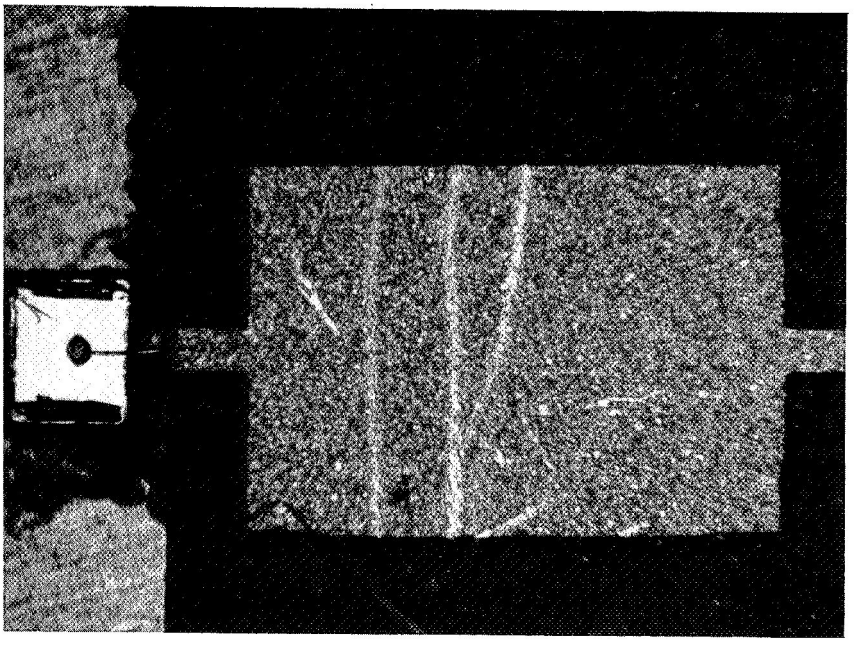

(b)

6915-21

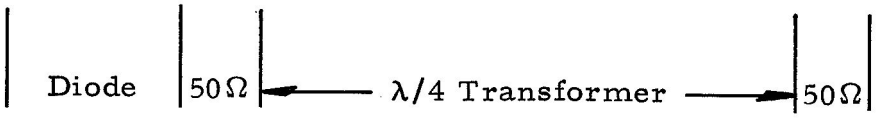

Figure 20 Photographs of Microstrip Circuit.
(a) Overall view, (b) diode placement.

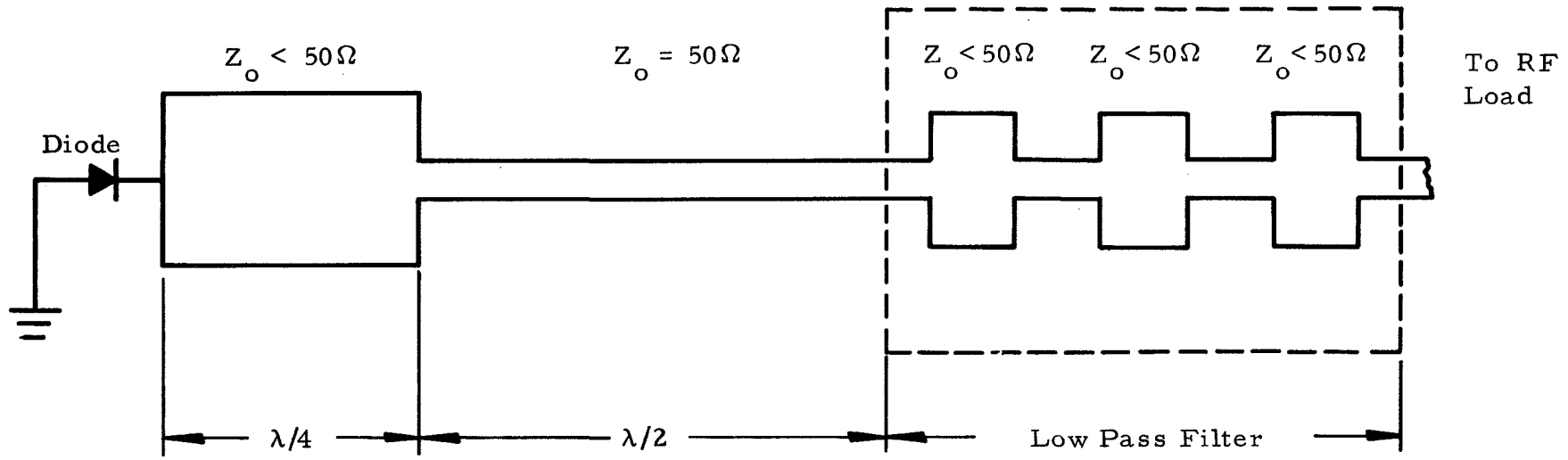

Figure

Figure 21 Proposed TRAPATT Microstrip Circuit

SECTION IV

SUMMARY

We have successfully operated GaAs avalanche diodes in the IMPATT mode in microstrip circuits and have met most of the NASA requirements for a solid state microwave source for satellite communications. While we have not yet been able to operate our diodes in the high efficiency TRAPATT mode, we believe that such operation is possible. Because diodes which are fabricated for TRAPATT operation must have epitaxial n-layers that are thin enough to permit "punch-through," they are highly susceptible to tuning induced failures. Imperfections are always present at the substrate-epitaxial layer interface, and if this interface is subjected to a high electric field, failures are likely. The intermediate epitaxial n^+ layer that we now grow on the substrate prior to growth of the n-layer serves to remove the substrate from the high field region. This should make it possible to operate these diodes in the TRAPATT mode in an appropriately designed circuit.

REFERENCES

1. G. I. Haddad, P. T. Greiling, and W. E. Schroeder, "Basic Principles and Properties of Avalanche Transit-Time Devices," IEEE Trans. - Microwave Theory and Tech. MTT-18, 752 (1970).

2. A. S. Clorfeine, R. J. Ikola, and L. S. Napoli, "A Theory for the High-Efficiency Mode of Oscillation in Avalanche Diodes," RCA Review 30, 397 (1969).

3. D. W. Shaw, "Kinetics of Transport and Epitaxial Growth of GaAs with Ga-$AsCl_3$ System," J. Crystal Growth 8, 117 (1971).

4. M. S. Abrahams and C. J. Buiocchi, "Etching of Dislocations on the Low Index Faces of GaAs," J. Appl. Phys. 36, 2855 (1965).

5. R. H. Haitz, H. L. Stover, and N. J. Tolar, "A Method for Heat Flow Resistance Measurements in Avalanche Diodes," IEEE Trans. - Electron Devices ED-16, 438 (1969).

6. J. W. Gewartowski and J. E. Morris, "Active IMPATT Diode Parameters Obtained by Computer Reduction of Experimental Data," IEEE Trans. - Microwave Theory and Tech. MTT-18, 157 (1970).

7. M. V. Schneider, "Microstrip Lines for Microwave Integrated Circuits," Bell System Tech. J. 48, 1421 (1969).

APPENDIX

SUPPORT FOR K_u-BAND GUNN LOCAL OSCILLATOR PROGRAM

APPENDIX

SUPPORT FOR K_u-BAND GUNN LOCAL OSCILLATOR PROGRAM

The GaAs Schottky barrier diodes developed in this program have proved to be instrumental in satisfying government requirements for a K_u-band local oscillator which is being developed in the Equipment Group at Texas Instruments. This work is being done in the Central Research Laboratories by Dr. D. N. McQuiddy, who is on assignment from the Equipment Group.

The local oscillator consists of a Gunn diode oscillator with a varactor diode for electronic tuning. We found that commercially available silicon and GaAs varactor diodes do not provide tuning which meets the required specifications over the temperature range from -55°C to +75°C.

We supplied GaAs Schottky barrier diodes for use as tuning varactors. Using these diodes, it was possible for Dr. McQuiddy to design a tuning structure which exceeded the specifications for the local oscillator program. We tailored the zero bias capacitance and microwave package configuration to meet his requirements. The actual oscillator performance exceeded the specifications over the required temperature range. The results are:

(1) 100 mHz electronic tuning range at 15 mHz/V.

(2) Linear tuning rate: < 0.5 dB power variation over the 100 mHz range.

(3) Performance maintained within a frequency band of 16.3 to 16.7 GHz.